Developing resilience pathways for interdependent infrastructure networks

A simulation-based approach with consideration to risk preferences of decision-makers

Balakrishnan, Srijith; Jin, Lawrence; Cassottana, Beatrice; Costa, Alberto; Sansavini, Giovanni

DOI
10.1016/j.scs.2024.105795

Publication date
2024

Document Version
Final published version

Published in
Sustainable Cities and Society

Citation (APA)
Balakrishnan, S., Jin, L., Cassottana, B., Costa, A., & Sansavini, G. (2024). Developing resilience pathways for interdependent infrastructure networks: A simulation-based approach with consideration to risk preferences of decision-makers. *Sustainable Cities and Society*, *115*, Article 105795. https://doi.org/10.1016/j.scs.2024.105795

Sustainable Cities and Society 115 (2024) 105795

Contents lists available at ScienceDirect

Sustainable Cities and Society

journal homepage: www.elsevier.com/locate/scs

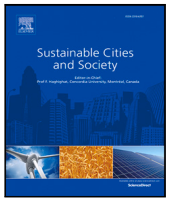

Developing resilience pathways for interdependent infrastructure networks: A simulation-based approach with consideration to risk preferences of decision-makers

Srijith Balakrishnan [a,*], Lawrence Jin [b], Beatrice Cassottana [c], Alberto Costa [c], Giovanni Sansavini [d]

[a] Faculty of Technology, Policy and Management, Delft University of Technology, Jaffalaan 5, 2628 BX Delft, The Netherlands
[b] Lee Kuan Yew School of Public Policy, National University of Singapore, 469C Bukit Timah Rd, 259772, Singapore
[c] Global Infrastructure Basel Foundation, Elisabethenstrasse 28, 4051, Basel, Switzerland
[d] Reliability and Risk Engineering, ETH Zürich, LEE K 225 Leonhardstrasse 21, 8092 Zürich, Schweiz, Switzerland

ARTICLE INFO

Dataset link: GitHub, https://github.com/srijithbalakrishnan/dreaminsg-integrated-model, 4TU.ResearchData

Keywords:
Infrastructure simulation
Interdependencies
High-impact low-probability
Cumulative prospect theory
Resilience

ABSTRACT

In this study, we propose a methodological framework to identify and evaluate cost-effective pathways for enhancing resilience in large-scale interdependent infrastructure systems, considering decision-makers' risk preferences. We focus on understanding how decision-makers with varying risk preferences perceive the benefits from infrastructure resilience investments and compare them with upfront costs in the context of high-impact low-probability (HILP) events. First, we compute the costs of interventions as the sum of their capital costs and maintenance costs. The benefits of the interventions include the reduction in physical damage costs and business disruption losses resulting from the improved resilience of the network. In the final stage, we develop statistical models to predict the perceived net benefits of different network resilience configurations in power, water, and transport networks. These models are employed in an optimization framework to identify optimal resilience investment pathways. By incorporating Cumulative Prospect Theory (CPT) in the optimization framework, we show that decision-makers who assign higher weights to low probability events tend to allocate more resources towards post-disaster recovery strategies leading to increased resilience against HILP events, like earthquakes. We illustrate the methodology using a case study of the interdependent infrastructure network in Shelby County, Tennessee.

1. Introduction

Increasing extreme events and rapid expansion of urban regions have triggered a strong interest in infrastructure resilience building. Often, the higher-order effects of infrastructure disruptions resulting from localized events span across administrative and geographic boundaries, leading to significant socio-economic repercussions (Rinaldi, Peerenboom, & Kelly, 2001). These trends emphasize the need for significant investment to address physical and operational vulnerabilities and minimize disruptions to urban infrastructure systems in the event of large-scale exogenous shocks, such as natural disasters (Hallegatte, Rentschler, & Rozenberg, 2019). According to a report by the Organization for Economic Co-operation and Development (OECD) in 2018, an annual investment of US$6.9 trillion until 2050 is needed to support infrastructure development, achieve sustainable development objectives, and promote a low-carbon, climate-resilient future (OECD, The World Bank, & U.N. Environment, 2018). While prioritizing investment in regions with infrastructure deficiency is crucial, transforming existing infrastructure systems into more resilient ones is equally important.

Infrastructure resilience encompasses the ability of systems to anticipate, resist, absorb, respond to, adapt to, and recover from disturbances (Carlson et al., 2012). Given the increasing importance of infrastructure resilience in recent decades, the strategic allocation of resources to enhance resilience has become a critical component of modern infrastructure planning (Esmalian et al., 2022). This allocation of limited resources is pivotal in optimizing investments and ensuring the most effective protection of critical infrastructure systems against various potential disruptions. Historically, Cost–Benefit Analysis (CBA) has played a central role in influencing decision-making regarding infrastructure resilience (Pagliara & Zingone, 2023; Wise, Capon, Lin,

* Corresponding author.
E-mail addresses: s.balakrishnan@tudelft.nl (S. Balakrishnan), ljin@nus.edu.sg (L. Jin), beatrice.cassottana@gmail.com (B. Cassottana), alberto.costa@sec.ethz.ch (A. Costa), sansavig@ethz.ch (G. Sansavini).

https://doi.org/10.1016/j.scs.2024.105795
Received 18 March 2024; Received in revised form 5 August 2024; Accepted 2 September 2024
Available online 16 September 2024

Nomenclature

List of Notations

α, β	Parameters in value function of Cumulative Prospect Theory (CPT) to describe risk attitudes
β_{n_i}	Model coefficient corresponding to the resilience intervention n_i
ℓ	Seismic source, $\ell \in L$
η_p	Resilience factor corresponding to power services
η_w	Resilience factor corresponding to water service
γ	Parameter to specify the extent of overweighting in CPT
λ	Loss aversion coefficient in the CPT value function
$\mathbb{C}$	Total budgetary outlay for resilience enhancement across all infrastructure systems
$\mathbf{G}$	Aggregate prospect of resilience investments considering all potential hazard events (earthquakes)
$\mathcal{N}(\cdot)$	Normal distribution
$\mathcal{P}_\ell$	Percentage contribution of seismic source ℓ to the hazard
$\mathcal{P}_{M,\ell}$	Percentage contribution of a seismic rupture of magnitude M originating from source ℓ to the hazard
$\mathcal{P}_{M\|\ell}$	Conditional percentage contribution of a rupture of magnitude M within the source ℓ to the hazard
μ_R	Mean time for component recovery in days
ν^d	Damage ratio corresponding to damage state d
$\omega_{n_i,t}$	Percentage share of annual resilience budget allocated to intervention n_i in the year t
$\Phi(\cdot)$	Standard normal cumulative distribution
$\pi^{\pm}$	Decision weights in CPT
ρ	Reinforcement factor which indicates the fraction of replacement cost to upgrade the component to a certain level of resilience
σ_R	Standard deviation of time for component recovery in days
θ_d	Median of the intensity measure corresponding to damage state d
φ_d	Standard deviation of the natural logarithm of the intensity measure IM corresponding to damage state d
ξ	Model exponent to capture the concave relationship between resilience prospect and budget allocation
a	Service area dependent on a unique pair of water and power demand nodes, $a \in A$
B	Total benefit of a resilience investment considering loss reduction to physical infrastructure and business operations
C^s	Total cost of resilience investment for upgrading from base resilience configuration to the configuration s
C_{res}	Total cost for post-disaster manpower and equipment
C_{rob}	Total cost for reinforcing infrastructure components
C_t	Resilience budget for all infrastructure systems for the year t of the investment period
d	Damage state of a component, d
DL	Damage loss of infrastructure components or systems
EL	Economic loss due to business disruptions
EOH_p	Equivalent outage hours corresponding to power services
EOH_w	Equivalent outage hours corresponding to water services
F_d	Fragility function corresponding to damage state d
G	Prospect of outcomes according to CPT
h	Hazard event, $h \in H$
I^s	Set of infrastructure components to be upgraded to achieve a resilience level s
IM	Intensity measure
k	Economic sector, $k \in K$
M	Magnitude of the earthquake
n_i	Resilience intervention type, $0 \le i \le N$
O	Annual economic output
p^s	Ratio of cost for improving resourcefulness to replacement cost of the network
P_e	Probability of exceedance of an event
P_h	Annual probability of occurrence of an seismic rupture event
P_i	Probability of outcome i in CPT
r	Discount rate
s	Network resilience configuration, $s \in S$
T	Time period for which a hazard is to be characterized
T_D	Design period for the resilience enhancement project
T_I	Investment period for the resilience enhancement project
T_{RP}	Return period of an event in years
T_R	Recovery/restoration time of an infrastructure component
$v(x)$	Value function in CPT
$w(h)$	Weight assigned to an event h; it depends on the probability of hazard event h
$w^{\pm}$	Decision weighting functions in CPT

& Stafford-Smith, 2022). This approach evaluates potential investments by comparing upfront and maintenance costs with anticipated long-term benefits. While it is effective for evaluating common and recurring events, the limitations of this analysis become apparent when dealing with high-impact low-probability (HILP) disaster events, which are of significant concern from a resilience perspective (Panteli & Mancarella, 2017).

The core issue lies in the rarity and catastrophic potential of HILP events, such as earthquakes of immense magnitude or unprecedented superstorms. The concept of expected annual loss, which involves the cumulative sum of all potential disaster losses weighted by their

annual occurrence probabilities, is frequently employed in CBA calculations (Mechler, 2016). An unintended consequence of this approach is that relatively lower-impact higher-probability events tend to dominate risk assessments, while the consequences of extreme events with very low chances of occurrence make a small contribution to the expected losses (Merz, Elmer, & Thieken, 2009). This can be especially problematic when there are large uncertainties in the likelihood and consequences of future HILP events. These parameters, when estimated from past observational data, may fail to fully account for all possible HILP events as well as the full extent of their consequences. As a result, a risk-neutral decision-maker may fail to accurately consider the full range of consequences posed by HILP events in traditional CBA.

At the same time, decision-makers are not always rational in their behavior. A large and growing literature in behavioral economics and prospect theory suggests that decision-makers often exhibit risk preferences that deviate from rationality (Altman, 2010). For example, people tend to be loss averse; risk-seeking in the loss domain and risk-averse when they see a chance of gains; and importantly, they tend to overweight low probabilities and underweight high probabilities (Barberis, 2013; Kahneman & Tversky, 1979). As a result, compared to risk-neutral decision-makers, prospect theory decision-makers may assign greater importance to HILP events when evaluating resilience investment alternatives. In the context of resource allocation for resilience, it is of considerable interest to understand how different risk preferences of the decision-maker can impact investment decisions, especially in consideration of high-impact low-probability events.

In this study, we introduce a integrated framework to investigate the effect of risks preferences of decision-makers on their resource allocation pathways towards enhancing the collective resilience of interdependent infrastructure networks in the context of HILP events. Pathways represent the decisions about resource allocation to various resilience interventions during the multi-year implementation phase. The specific objectives of the study are as follows:

1. Develop an integrated infrastructure-industry simulation model to capture the role of disaster-induced infrastructure disruptions on economic sectors.
2. Develop target resilience levels for the infrastructure components in the interdependent network by formulating incremental changes to resilience capabilities (pre-disaster robustness and post-disaster recovery).
3. Develop resilience investment pathways for the interdependent network by formulating an optimization problem that maximizes 'perceived' net benefits of resilience investments over the design horizon.
4. Incorporating Cumulative Prospect Theory in the methodology, investigate how decision-makers with varying risk preferences (probability weighting preferences) perceive the net benefits from infrastructure resilience interventions and their role on resource allocation pathways.

The subsequent sections of the paper are structured as follows: Section 2 presents a concise overview of resource allocation decision-making approaches and methods for embedding risk preferences; Section 3 discusses the methodological framework for developing pathways to enhance the resilience of interdependent infrastructure networks; Section 4 presents an application of the proposed methodology on a case study involving the interdependent power, water, and transport network in Shelby County, Tennessee (U.S.); and finally, Section 5 summarizes the paper's findings and conclusions.

2. Background

2.1. Disaster risks to infrastructure systems and the need for resilience

Critical infrastructure systems play a vital role in cities by supporting economic activities, sustaining communities, and promoting societal well-being. However, the increasing complexity and interdependence of critical infrastructure systems have made them more vulnerable to disaster events (Ouyang, 2014). The consequences of disaster-induced infrastructure damages and disruptions extend beyond physical damage, resulting in significant socioeconomic losses. Chang (2016) classified these higher-order effects into four categories, namely, health, social, economic, and environmental consequences (Chang, 2016).

One of the key contributors to the propagation of infrastructure failure effects to other systems is the increasing level of interdependencies. Urban infrastructure networks, consisting of transportation, energy, water, telecommunications, and more, are tightly intertwined through physical, logical, cyber, and geographic dependencies (Rinaldi et al., 2001). While these interdependencies are inevitable for improving operational efficiency and coordination, they can become major sources of higher-order vulnerability during exogenous shocks. The interdependencies create a 'domino effect' during crises, where the failure of one system triggers failures of other systems, and escalates to larger geographical regions affecting significantly large populations and economies (Wang, Hong, & Chen, 2012).

Critical infrastructure risks may not necessarily emanate from the vulnerability of existing infrastructure systems alone; the changing hazard profiles and spatial dynamics also contribute to the increasing risks. Climate change intensifies the frequency and severity of extreme weather events and thereby increases the exposure (Güneralp, Güneralp, & Liu, 2015). This is further exacerbated by land use changes and population growth in these regions of high hazard exposure. A recent study by Rentschler et al. (2023) revealed that human settlements in hazardous flood zones have surpassed those in flood-safe zones by up to 60% since 1985, particularly in regions like East Asia (Rentschler et al., 2023).

While the importance of ensuring adequate resilience of infrastructure systems is indisputable, it is equally crucial to improve our understanding of how resilience can be achieved. Infrastructure resilience can be broadly defined as the ability of an infrastructure system to withstand a change or a disruptive event and minimize further performance deviations (Nan & Sansavini, 2017). Resilience frameworks, such as the $4R's$ framework (in which resilience is characterized as robustness, redundancy, resourcefulness, and rapidity capabilities) (Bruneau et al., 2003), *absorb-adapt-transform* framework (Béné, Wood, Newsham, & Davies, 2012) and the *absorb-restore-adapt* framework (Francis & Bekera, 2014) classified infrastructure resilience interventions into resilience characteristics and provided practical insights into infrastructure resilience enhancement. Recent studies also incorporate concepts, such as, preventive, anticipative, and transformative capabilities as essential qualities of a resilient infrastructure system (Manyena, Machingura, & O'Keefe, 2019).

2.2. Cost–Benefit Analysis (CBA) for infrastructure (resilience) investments

Cost–Benefit Analysis (CBA) is a widely adopted framework to evaluate infrastructure projects, policies, and decision alternatives (Chi & Bunker, 2021; Jones, Moura, & Domingos, 2014). It primarily focuses on assessing the costs and benefits associated with a particular course of action. In CBA, the costs and benefits associated with a project or decision are quantified and expressed in monetary terms. The analysis aims to determine whether the benefits derived from the project outweigh the costs incurred. To account for the time value of money, future costs and benefits are discounted.

The central equation in CBA is the net present value (NPV) formula, which calculates the present value of the net benefits. The NPV is expressed $NPV = \sum_{t=0}^{T}(B_t - C_t)/(1+r)^t$ where B_t represents the benefits in time period t, C_t represents the costs in time period t, r is the discount rate, and T is the time horizon of the analysis. The above relationship takes into account the timing of costs and benefits, and the discount rate reflects the opportunity cost of capital or the rate of return required

to compensate for the delay in receiving benefits or incurring costs. A positive NPV indicates that the benefits exceed the costs, suggesting that the project or decision is economically viable. Conversely, a negative NPV suggests that the costs outweigh the benefits, indicating that the project may not be economically justified. In addition to NPV, other metrics are also commonly used in Cost–Benefit Analysis, such as the benefit–cost ratio (BCR) and internal rate of return (IRR).

Chadburn et al. (2010) stated that cost–benefit analyses can be used to develop economic arguments in favor of risk reduction investments rather than responding to future disaster events (Chadburn, Jacobo, Kenst, & Venton, 2010). CBA is considered the most common approach for prioritizing infrastructure resilience upgrades (Hallegatte, Rozenberg, Rentschler, Nicolas, & Fox, 2019) and is capable of identifying risks and cost-effective risk reduction measures (Michel-Kerjan et al., 2013). For instance, Croope and McNeil (2011) developed a decision-support system based on CBA to compare societal, economic and physical interventions that can reduce vulnerability and improve recoverability of regions and critical infrastructure systems after disasters (Croope & McNeil, 2011). Zhu and Leibowicz (2022) applied CBA to determine the cost-effectiveness of power network hardening interventions against floods and winds (Zhu & Leibowicz, 2022).

Despite its wide adoption, CBA has faced significant scrutiny due to several practical limitations. Some of the criticisms of CBA as a decision-making tool for evaluating disaster risk reduction alternatives include its inability to represent HILP events in risks, the inability to capture intangible and indirect effects, and the inability to resolve conflicting objectives (Mechler, 2016). For instance, using a probabilistic approach to estimate risk reduction due to interventions would 'smooth' the benefits of actions aimed at reducing risks from very-low probability events, impacting the viability of such projects. In addition, CBA is also not suitable for accounting for benefits that are difficult to quantify in monetary terms and existing methods to mitigate them are often affected by value judgements (The World Bank, 2010) With respect to resource allocation for infrastructure resilience, McDonald et al. (2020) listed two distinct challenges for CBA, namely, its inability to handle HILP nature of natural hazards and the complex and interconnected nature of urban infrastructure networks that leads to network-wide effects of resilience interventions (McDonald, Timar, McDonald, & Murray, 2020). From a more practical perspective for decision-making, Shreve and Kelman (2014) observed that most of the risk reduction studies that adopt CBA framework do not report the costs and benefits of the various strategies to enable an informed understanding of their relative effectiveness in reducing the risks.

2.3. Accounting for risk preferences in infrastructure decision-making

While CBA offers a robust decision-making tool that assists decision-makers, it is incapable of explaining how various psychological factors that influence decision-makers' perceptions and valuations of costs and benefits. As far as resilience is concerned, how decision-makers perceive extreme risks has a significant influence on how they allocate resources to mitigate them. One of the key challenges with ascertaining the benefits of infrastructure resilience upgrades is the need to quantify the estimated reduction of risk in the form of an expected value. In a risk-neutral setup, the expected loss (or gain) is the sum of all consequences weighted by its probabilities. However, research has shown that decision-makers perceive probabilities differently (Gayer, 2010), and this can have an effect on the perceived loss (or) gain from an action. This will have consequences in the way they allocate resources for infrastructure resilience. Two major frameworks exist to capture the risk preferences of individuals in decision-making, namely, Expected Utility Theory (EUT) and Cumulative Prospect Theory (CPT).

EUT and CPT offer distinct perspectives on decision-making. EUT is a normative framework that focuses on maximizing expected utility by considering probabilities and subjective values (von Neumann & Morgenstern, 2007). In contrast, CPT is a descriptive model that accounts for psychological biases in risk preferences (Tversky & Kahneman, 1992). One key difference is how they handle decision-makers' bias towards low probabilities. Expected Utility Theory (EUT) assumes that individuals assess the utility of each potential outcome of a decision and make their choice based on the expected utility, which is calculated using the probabilities of these outcomes. These probabilities are treated as the true, objective probabilities of the outcomes. In contrast, CPT uses a weighting function that assigns higher weight to low probabilities. This accounts for the tendency of individuals to overestimate the likelihood of rare events and influences their decision-making process. Both frameworks are widely utilized for resource allocation to incorporate decision-makers' risk preferences in infrastructure investment decision, namely, asset management (Gharaibeh, Chiu, & Gurian, 2006), infrastructure planning (Li et al., 2022; Scholten, Schuwirth, Reichert, & Lienert, 2015), infrastructure maintenance (Cheng & Frangopol, 2022; Porras-Alvarado, 2016), cyber-security of infrastructure systems (Yang, Kiekintveld, Ordonez, Tambe, & John, 2011), and disaster resilience (Cha & Ellingwood, 2012). A review of the above two frameworks is presented in Appendix A.1.

2.4. Gaps in the literature and contribution

While risk-based assessments and cost–benefit analyses provide valuable insights into resilience investments, they may not fully capture the complexity of HILP events. HILP events can have far-reaching consequences that ripple through interconnected infrastructure systems, causing systemic failures that exceed the scope of traditional risk assessments (McDonald et al., 2020). Traditional risk-neutral approaches often underestimate the impacts of rare and catastrophic events, leading to inadequate resource allocation for enhancing resilience against HILP events (Panteli & Mancarella, 2017). However, it is important to recognize that decision-makers are not always risk-neutral or rational in their decision-making processes. Their treatment of HILP events can vary significantly, resulting in diverse resource allocations. Given the flexibility of CPT in handling low-probability events differently (Tversky & Kahneman, 1992), it can be used to model the risk preferences of decision-makers towards HILP events better than other behavioral models. By considering decision-makers' attitudes towards risks from low-probability events using CPT, we can better understand how these preferences shape resource allocation strategies and their implications for enhancing the collective resilience of urban infrastructure systems in the face of HILP events.

3. Methodology

Fig. 1 illustrates the methodological framework adopted in the study. First, the seismic hazard in the study region is characterized, and an earthquake event set is created. Later, the infrastructure network failures and subsequent business disruptions due to each of the earthquake scenarios of interest are simulated under various network resilience configurations using an integrated simulation model. Subsequently, the decision-makers' perceptions (behavioral aspects) on the benefit from resilience interventions are statistically modeled using the simulation dataset. Finally, the statistical models are embedded in an optimization framework to derive and analyze the resilience pathways adopted by decision-makers with divergent risk preferences. The methodology is operationalized in five sequential stages, namely, (a) modeling of hazard and infrastructure component vulnerability, (b) simulation of interdependent effects of infrastructure disruptions (c) quantification of indirect impacts on economic sectors due to business disruptions, (d) development of statistical models to predict gains from resilience investments including those from HILP events, and (e) development of optimal resilience pathways. While the methodology is developed for adapting infrastructure systems against earthquake hazard, it can be applied to any type of hazard or multi-hazards.

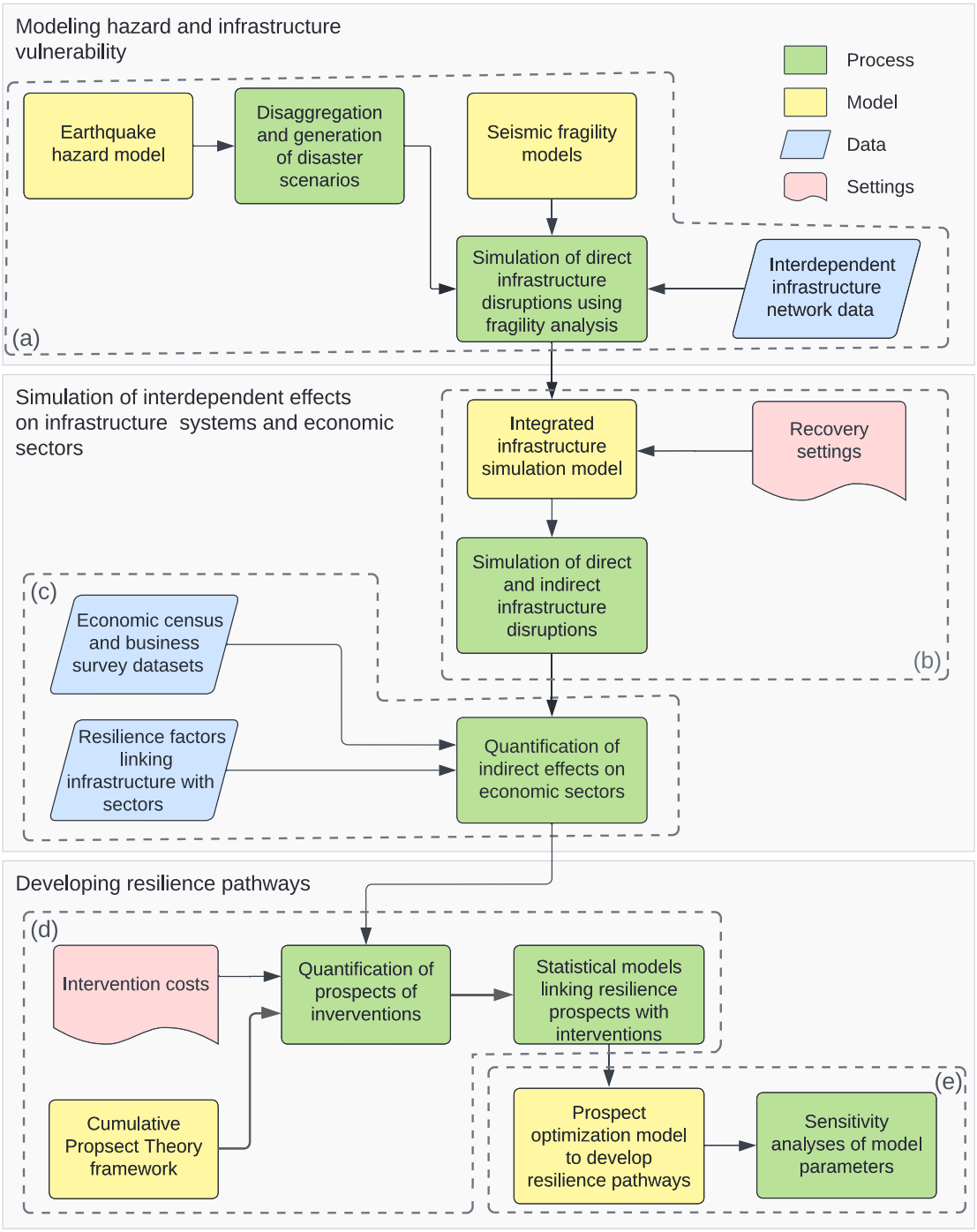

Fig. 1. Methodology for developing optimal infrastructure resilience pathways.

3.1. Hazard modeling and characterization

In this study, OpenQuake Engine (Pagani, Monelli, Weatherill, Danciu, et al., 2014), an open-source seismic risk analysis platform, is used to simulate earthquake events. We adopted an event-based method where we identified earthquake rupture scenarios that go beyond the exceedance probability threshold predefined by the decision-maker. The seismic intensities are characterized using the concept of return periods. The process begins by choosing an investigation period (in years) and a target ground motion parameter of interest (for example, peak ground acceleration (PGA), peak ground velocity (PGV) and peak ground displacement (PGD)). A disaggregation analysis is conducted to identify the seismic sources that exceed a probability threshold and quantify their contribution to the overall hazard (Pagani, Monelli, Weatherill, Danciu, et al., 2014). The disaggregation is then performed for the selected sources to obtain the conditional probability of exceedance by magnitude and the contribution of each rupture scenario. Finally, the chosen rupture scenarios are simulated using ground motion models to evaluate parameters like peak ground acceleration, velocity, and displacement across the study region. The detailed step-wise methodology to develop the earthquake event set and corresponding ground motion fields are presented in Appendix A.2.

3.2. Vulnerability and recovery modeling of infrastructure components

The direct damages incurred by different infrastructure components, such as pipelines, power lines, and road links, as a result of earthquake events, are modeled using fragility functions (Federal Emergency Management Agency, 2020). Discrete damage states are defined based on the continuous extent of damage to the infrastructure components. Each damage state is described by a fragility function $F_d(IM)$, which represents the probability of surpassing the damage level $D = d$ for a given intensity measure $IM = x$ (Eq. (1)).

$$F_d(IM) = P[D \geq d | IM = x] = \Phi\left[\frac{1}{\varphi_d} \ln \frac{x}{\theta_d}\right] \quad (1)$$

where $\Phi[\cdot]$ is the standard normal cumulative distribution, φ_d is the standard deviation of the natural logarithm of the intensity measure corresponding to the damage state d and θ_d is the median of the intensity measure corresponding to d.

At the same time, the recovery periods of infrastructure components are modeled using a normal distribution of restoration periods (Eq. (2)).

$$T_R = \mathcal{N}\left(\mu_R, \sigma_R^2\right) \quad (2)$$

where T_R is the time of recovery of an infrastructure component, μ_R is the mean time of recovery, and σ_R is its standard deviation.

The direct damage to infrastructure components and the subsequent recovery process due to other hazards can also be modeled in a similar fashion by using corresponding fragility functions and recovery distributions specific to them.

3.3. Interdependent infrastructure simulation

We used InfraRisk, an integrated power-water-transport simulation model, to simulate the network-wide effects of infrastructure disruptions induced by the seismic events (Balakrishnan & Cassottana, 2022). InfraRisk achieves interdependent infrastructure simulation by integrating infrastructure-specific models through an object-oriented interface. This integration involves identifying and modeling the dependencies among different infrastructure components and ensuring time synchronization among the infrastructure simulation models. The details of various modules in the integrated simulation model is provided in Appendix A.3. The temporal functional changes to infrastructure components due to disaster impacts and recovery are captured using resilience metrics derived from the concept of satisfied demand (ratio of supply to demand). These resilience metrics can be designed by considering a number of criteria, such as performance, equity, accessibility, among others. In this study, the water and power disruptions at the demand nodes are quantified as Equivalent Outage Hours (EOH_w and EOH_p, respectively).

3.4. Quantification of effects of infrastructure disruptions on regional economic sectors

Infrastructure service disruptions can have significant impacts on the operational continuity of dependent businesses, as extensively documented in the literature. In this study, we incorporated business losses resulting from infrastructure disruptions into the resilience decision-making framework.

To simulate business disruptions caused by infrastructure failures, links are established between the interdependent infrastructure model and the industrial sectors dependent on it. The interdependent infrastructure simulation model captures the spatio-temporal variations in water and power supply at the respective demand nodes. By delineating the service areas for each demand node, the businesses dependent on these nodes are mapped in a sector-wise manner. Spatial datasets on economic activities at local, regional, and national levels are routinely collected by many countries, such as the United States, through periodic censuses and surveys. Leveraging these datasets, which include information such as economic output, the economic activities can be scaled down to their respective service areas based on metrics such as sector-wise employee size and the total number of business units.

In the literature, two approaches have been employed to establish the link between infrastructure failures and business disruptions. The first approach utilizes technical coefficients derived from input–output (IO) tables to quantify the initial shock to economic sectors resulting from infrastructure disruptions (Haimes et al., 2005; Santos, 2006). However, this approach has limitations as the technical coefficients primarily capture economic relationships between sectors rather than functional dependencies. The second approach involves conducting surveys to quantify the functional dependencies of businesses on infrastructure services. These surveys provide insights into the sector-specific percentages of operability (resilience factors) immediately after disruptions to water and power services, among others (Chang, Seligson, & Eguchi, 1996; Kajitani & Tatano, 2009). In this study, the resilience factors reported by Kajitani and Tatano (2009) are adopted to establish the link between water and power network disruptions and business output.

In particular, η_p, η_w are the power and water resilience factors, which indicate the functional level of sector $k \in K$ of the economy due to power disruption and water disruption, respectively. If the annual output from sector k within an area a dependent on a pair of water and power demand nodes is O_a^k, then the total economic loss contributed by k in a is given by Eq. (3).

$$EC_a^k = \frac{1}{365 \times 24}\left[(1-\eta_p)EOH_p^a + (1-\eta_w)EOH_w^a\right] \times O_a^k \quad (3)$$

where EOH_p^a and EOH_w^a are the equivalent outage hours corresponding to power and water disruptions resulting from a seismic event in area a. Then, the cumulative economic impact due to the event can be calculated as in Eq. (4).

$$EC = \sum_{a \in A} \sum_{k \in K} EC_a^k \quad (4)$$

where A is the set of all service areas and K is the set of all economic sectors.

3.5. Costs and benefits of resilience interventions

A wide range of resilience alternatives can be proposed for water, power, and transport systems. These alternatives may include reinforcing above-ground water tanks, strengthening power transmission towers and transformers, and increasing the availability of repair crews, among others. In this study, the focus is on two specific categories of resilience interventions, namely, those aimed at enhancing robustness and those meant to improve the resourcefulness of the systems. Robustness refers to the absorptive capacity of an infrastructure system whereas resourcefulness is directly linked to post-disaster recoverability and adaptability. Each intervention incurs a cost but effectively reduces the collective impact of disaster events on the interdependent infrastructure network and its dependent businesses.

To simplify computational complexity, we conducted cost–benefit calculations for ‘network resilience configurations’ instead of individual interventions. A network resilience configuration is defined as a combination of individual resilience interventions (upgrades) applied to different infrastructure components, collectively improving the resilience of the interdependent infrastructure network to a certain degree. The objective of the cost–benefit calculations is to determine whether the perceived benefits of a network resilience configuration outweigh the initial costs associated with it.

For the cost–benefit calculation, the following costs are taken into consideration:

1. The cost of implementing robustness interventions before a disaster event. Robustness is improved by reinforcement, retrofitting, or replacement of existing infrastructure components.

2. The cost of enhancing resourcefulness ans rapidity during and after a disaster event. Resourcefulness and rapidity are improved through investments in post-disaster recovery crews and equipment.

The benefits of resilience interventions can be of two types as follows:

1. Reduction in physical repair/replacement costs compared to a do-nothing strategy for the given set of disaster events.
2. Reduction in economic losses incurred by businesses due to infrastructure disruptions.

The rest of the section provides a detailed description of the methods employed to quantify the costs and benefits associated with resilience configurations.

3.5.1. Calculation of costs

Given that the interventions are determined prior to the occurrence of a disaster, the corresponding costs are calculated for network resilience configurations.

Let us assume that the full replacement cost of component i under base configuration s_0 is RC_i. The base resilience configuration, s_0, denotes the current resilience capabilities of the network before resource allocation. We define a reinforcement factor corresponding to resilience configuration s as $\rho_i^s : \rho_i^s \geq 0$, which is the fraction of the replacement cost that would be needed to reinforce i. If $I^s \ni i$ is the set of components to be reinforced to attain a resilience configuration s, then the total cost of reinforcement is given by Eq. (5).

$$C_{rob}^s = \sum_{i \in I^s} \rho_i^s RC_i \tag{5}$$

The cost of resourcefulness and rapidity enhancement is calculated as the sum of the additional investment in improving maintenance and restoration capacity. The cost of interventions aimed at improving resourcefulness and rapidity is primarily associated with manpower and equipment. These costs can be quantified as a proportion (ϱ^s) of the replacement cost of the network under the base resilience configuration s_0 (Eq. (6)).

$$C_{res}^s = \varrho^s RC_{net} \tag{6}$$

where $\varrho^s > 0$ and $RC_{net} = \sum_{i \in net} RC_i$ is the total replacement cost of the network considering all components.

The total cost of resilience investment corresponding to the configuration s is therefore given by the following equation (Eq. (7)).

$$C^s = C_{rob}^s + C_{res}^s \tag{7}$$

3.5.2. Calculation of benefits

We consider several resilience configurations denoted by $s \in S$. The benefits should be calculated for all possible hazard events $h \in H$. Each hazard event h may inflict a certain level of damage on the exposed infrastructure components. The damage of a component i is characterized using discrete damage states $d \in D$ (Eq. (8)).

$$d = f(h, s) \tag{8}$$

where $f(\cdot)$ is the functional form of the component fragility curve.

The damage cost corresponding to each damage state is assumed to be proportional to the replacement cost of the component RC_i and is given by Eq. (9).

$$DL_i^{h,s} = v_i^{d(h,s)} RC_i \tag{9}$$

where $v_i^{d(h,s)}$ is the damage ratio of component i corresponding to damage state d resulting from a hazard h under configuration s and $0 \leq v_i \leq 1$.

The total cost of replacement/repair of the whole network if configuration s is implemented corresponding to hazard event h is (Eq. (10)):

$$DL_{net}^{h,s} = \sum_{i=1}^{n} DL_i^{d(h,s)} \tag{10}$$

The total damage loss to the entire network for the base resilience configuration s_0, i.e. under the do-nothing strategy, is denoted as DL_{net}^{h,s_0}. Therefore, the effective reduction in damage loss resulting from the implementation of replacement and repair measures can be expressed as shown in Eq. (11).

$$\Delta DL_{net}^s = DL_{net}^{h,s} - DL_{net}^{h,s_0} \tag{11}$$

The other benefit of resilience interventions stems from the reduction in economic losses from business disruptions, owing to upgrading to network resilience configuration s. The total direct economic loss due to an event h incurred by each sector k of the economy under resilience configuration s is denoted as $EL_k^{h,s}$. The total direct economic loss caused by the network interruptions is given by Eq. (12).

$$EL^{h,s} = \sum_k EL_k^{h,s} \tag{12}$$

The total economic disruption due to hazard event h under a do-nothing strategy is EL^{h,s_0}, and the effective reduction in costs resulting from replacement and repair measures can be calculated as shown in Eq. (13).

$$\Delta EL^{h,s} = EL^{h,s} - EL^{h,s_0} \tag{13}$$

Consequently, the total benefits corresponding to event h due to the implementation of configuration s are calculated as follows (Eq. (14)):

$$B^{h,s} = \Delta DL_{net}^{h,s} + \Delta EL^{h,s} \tag{14}$$

3.6. Incorporating risk attitudes of decision-makers using Cumulative Prospect Theory

CPT is employed to gain insight into how decision-makers overweight or underweight HILP events in the resource allocation process. To apply CPT, the assumption is made that each seismic event occurs independently of others. In other words, in a given year, there can be ruptures of different magnitudes originating from the same source. Since each seismic event has only two possible outcomes (either the earthquake event occurs in a year or it does not), the estimation of potential gains from investing in a resilience intervention needs to take into account these two possible outcomes.

Consider an earthquake event h with annual probability of occurrence P_h. Let us also assume that the current base resilience configuration s_0 entails the lowest resilience. We can improve the resilience to the resilience target configuration s by investing C^s resources. This will lead to a loss reduction of $B^{h,s}$ if the event h occurs. If the earthquake does not occur (denoted by h'), the loss reduction is zero. According to CPT (Tversky & Kahneman, 1992), the decision weights of the above outcomes are (Eqs. (15) and (16)):

$$\pi_h^+ = \frac{P_h^\gamma}{\left(P_h^\gamma + (1-P_h)^\gamma\right)^{\frac{1}{\gamma}}} \tag{15}$$

$$\begin{aligned} \pi_{h'}^+ &= \frac{\left[(1-P_h)+P_h\right]^\gamma}{\left(\left[(1-P_h)+P_h\right]^\gamma + (1-[(1-P_h)+P_h])^\gamma\right)^{\frac{1}{\gamma}}} \\ &\quad - \frac{(1-P_h)^\gamma}{\left((1-P_h)^\gamma + (1-(1-P_h))^\gamma\right)^{\frac{1}{\gamma}}} \\ &= 1 - \frac{(1-P_h)^\gamma}{\left[(1-P_h)^\gamma + P_h^\gamma\right]^{\frac{1}{\gamma}}} \end{aligned} \tag{16}$$

where $\gamma \in [0,1]$ is the amount of over- or underweighting by the decision-maker. $\pi^{+}_{h'}$ represents the non-occurrence of the earthquake event in one year resulting in zero loss reduction from the resilience intervention and, therefore, the annual prospect (gain) share of the resilience investment due to event h can be calculated as in Eq. (17).

$$\begin{aligned} G^{h,s} &= \pi^{+}_{h} \times B^{h,s} + \pi^{+}_{h'} \times 0 \\ &= \pi^{+}_{h} B^{h,s} \end{aligned} \tag{17}$$

The cumulative annual prospect G^s of a resilience investment is the sum of the prospect contribution from all possible earthquakes in the event set H (Eq. (18)).

$$G^{s} = \sum_{h \in H} \pi^{+}_{h} B^{h,s} \tag{18}$$

The gains from each resilience intervention are different for decision-makers with varied risk preferences, and this can be easily investigated using CPT. In particular, when $\gamma = 1$, $\pi^{+}_{h} = P_h$, then G^s is the expected annual loss reduction due to the resilience investment, representing a risk-neutral and rational decision-maker as in EUT.

3.7. Development of optimal resilience pathways

In the subsequent phase, the costs and benefits linked to various network resilience configurations are leveraged to formulate budget allocation pathways aimed at achieving optimal resilience against seismic events. Each resilience configuration s represents a combination of resilience strategies implemented to specific degrees. By employing an integrated infrastructure-industry simulation model, the physical and economic repercussions resulting from each earthquake event h within the event set H are simulated, considering the various network resilience configurations $S \ni s$. With the simulated dataset, statistical models are constructed to predict the prospects for the design horizon T_D perceived by different types of decision-makers, based on the amounts invested in various resilience interventions. Linear regression models are used to develop these prediction models. The model specification used for the prediction models is presented in Eq. (19).

$$G = \beta_1 \left(C_1\right)^{\frac{1}{\xi}} + \beta_2 \left(C_2\right)^{\frac{1}{\xi}} + \cdots + \beta_N \left(C_N\right)^{\frac{1}{\xi}} \tag{19}$$

where G is the annual prospect (gain) from investing $C_1, C_2, \ldots, C_N$ amounts to $n_1, n_2, \ldots, n_N$ interventions. $n_1, n_2, \ldots, n_N$ represent subcategories of interventions that are aimed at improving robustness, resourcefulness, or rapidity capacities of the network. The model coefficients β_i are computed for decision-makers with different risk attitudes. Several studies have reported that resilience investments have diminishing marginal returns (Zhu & Leibowicz, 2022). This implies that the marginal gains for initial investments in all types of interventions are higher. The model exponent ξ (where $\xi \geq 1$) allows for a concave relationship between prospect gains and budget allocations. The regression models can predict the perceived gains from resilience investment combinations that vary in the budget allocated to different interventions.

While Eq. (19) captures the prospects resulting from resilience investments within a single year, it cannot be directly applied to resilience planning problems that involve budget allocations spanning multiple years. In such cases, where the total budget is fixed and distributed across the duration of the resilience project, i.e. the investment horizon T_I, optimizing the allocations across various types of resilience interventions becomes paramount. Thus, the subsequent phase of this study is aimed to address multi-year resilience enhancement projects as a resource allocation optimization problem. The underlying principle of this optimization approach is that there can exist different spending pathways to achieve a specific level of resilience; however, optimizing these pathways would ensure maximum perceived gain throughout the design period of the resilience project.

Let us consider a planned total budget $\mathbb{C}$, which is to be allocated uniformly over an investment horizon of T_I years, resulting in an annual investment of $C_t = \mathbb{C}/T_I$ for each year t within T_I. It is assumed that these investments contribute to the resilience of the infrastructure networks during the design horizon T_D, where $T_D \geq T_I$.

If we let n_i denote the set of resilience interventions in which C_t can be distributed, the investment proportions can be represented as $\omega_{n_i,t} \in \mathbf{W}$. Consequently, the annual investment in intervention n_i is given by $c_{n_i,t} = \omega_{n_i,t} C_t$. Eq. (20) presents the resource allocation optimization problem.

$$\begin{aligned} \max \quad & \mathbf{G} = \sum_{t'=1}^{T_I} \sum_{i=1}^{N} \beta_i \left[\sum_{t=1}^{t'} \frac{\omega_{n_i,t} C_t}{(1+r)^t} \right]^{\frac{1}{\xi}} + (T_D - T_I) \sum_{i=1}^{N} \beta_i \left[\sum_{t=1}^{T_I} \frac{\omega_{n_i,t} C_t}{(1+r)^t} \right]^{\frac{1}{\xi}} \\ \text{s.t.} \quad & \sum_{t=1}^{T_I} \sum_{i=1}^{N} \omega_{n_i,t} C_t \leq \mathbb{C} \\ & \forall t \in \{1, \ldots, T_I\} \qquad \sum_{i=1}^{N} \omega_{n_i,t} = 1 \\ & \forall i \in \{1, \ldots, N\} \qquad \sum_{t=1}^{T_I} \omega_{n_i,t} C_t \leq C^{max}_{n_i} \\ & \forall i \in \{1, \ldots, N\}, \forall t \in \{1, \ldots, T_I\} \quad 0 \leq \omega_{n_i,t} \leq 1 \\ & \forall t \in \{1, \ldots, T_I\} \qquad C_t = \frac{\mathbb{C}}{T_I} \end{aligned} \tag{20}$$

where $C^{max}_{n_i}$ is the maximum allowable budget for intervention n_i; r is the discount rate.

The objective is to maximize the perceived gains (prospect) throughout the design period of the project. The decision variables are the investment proportions $\omega_{n_i,t}$. The first term in the objective function represents the prospects of the annual investment in each intervention n_i over the investment horizon T_I. The second term in the objective function represents the prospects of the investment beyond the investment horizon T_I, i.e., during the remaining design horizon $T_D - T_I$. There are five constraints associated with the problem as follows:

1. Budget constraint: The total investment allocated over the investment horizon should not exceed the planned total budget $\mathbb{C}$.
2. Investment proportion constraint: For each year t within the investment horizon, the sum of investment proportions $\omega_{n_i,t}$ across all interventions n_i should be equal to 1. This ensures that the entire annual investment is allocated among the available interventions.
3. Maximum budget constraint: The sum of investments in each intervention n_i over the investment horizon should not exceed the maximum allowable budget $C^{max}_{n_i}$ for that intervention.
4. Investment proportion bounds: The investment proportions $\omega_{n_i,t}$ for each intervention n_i and year t should be within the range of 0 to 1, indicating the proportion of the annual investment allocated to that intervention.
5. Annual investment constraint: The annual investment C_t for each year t within the investment horizon is computed as the total budget $\mathbb{C}$ divided by the investment horizon T_I. This ensures an even distribution of investment over the years.

The above formulation is a nonlinear constrained optimization problem. As the above nonlinear optimization problem is convex[1] (a concave function is maximized), the optimal solutions can be found using a nonlinear solver like IPOPT (Wächter & Biegler, 2006). When $\xi = 1$, the problem is linear and the solver CPLEX (IBM ILOG, 2015) can be used.

[1] The relationship between prospects and investment is monotonously increasing.

The above optimization problem does not consider the feasibility of the investments at any year even though it maximizes for the corresponding perceived gains. We are also interested to know the year beyond which the cumulative investment costs for resilience interventions exceed the perceived gain. We identify the threshold year using Eq. (21).

$$\arg\min_{T} \sum_{t=1}^{T}\sum_{i=1}^{N} \omega_{n_i,t} C_t \geq \sum_{t'=1}^{T}\sum_{i=1}^{N} \beta_i \left[\sum_{t=1}^{t'} \frac{\omega_{n_i,t} C_t}{(1+r)^t}\right]^{\frac{1}{\xi}} \tag{21}$$

where $T : T \leq T_I$ is the threshold year within the investment horizon. The identification of the threshold year is performed separately because we are also interested in investigating the influence of risk preferences on the resource allocation by various decision-makers even if the solutions beyond the threshold year are infeasible.

4. Model application on Shelby County, Tennessee, United States

This section demonstrates the application of the proposed methodology on the well-known Shelby County interdependent infrastructure network. The case study investigated how decision-makers would allocate resources to different resilience interventions over the investment horizon of the project to improve the resilience of the interdependent network and thus reduce the overall physical and economic risks from seismic hazards in the region. In the process, we also explored how decision-makers with divergent risk preferences perceive the chances of occurrence of HILP events and its consequence on optimal resource allocation.

4.1. Shelby interdependent infrastructure network

The power and water networks, along with their corresponding service areas, are constructed using data obtained from Talebiyan and Duenas-Osorio (2020). The road transport network and transportation analysis zone datasets are collected from the TIGER/Line database of the U.S. Census Bureau and subsequently processed. The infrastructure network topologies are presented in Fig. 2.

The power network (Fig. 2(a)) comprises seventeen 23 kV substations, twenty 12 kV substations, 14 intersections, eight external grid connections, and 73 transmission lines connecting them. The total length of the network is approximately 369 km. The substations are considered as demand nodes from which power is distributed to businesses and households. Each substation has a unique service area. The water network (Fig. 2(b)) consists of the following components: six water tanks, nine pumping stations, 34 intersections, and 71 main pipelines, with a total length of 495 km. In the case of the water network, the intersections serve as demand junctions that provide water to their respective service areas. Due to a lack of micro-level data on the distribution networks of power and water networks, we assumed that all consumers within a service area are equally affected by a hazard event. For the transportation network (Fig. 2(c)), freeways, US highways, and urban and rural arterial roads are considered. The origin–destination flows are assigned using population estimates at the nodes.

Two types of interdependencies are taken into account during the construction of the interdependent infrastructure network. Firstly, the water pumps rely on the nearest substations for their power supply. If the substation is unable to provide sufficient power, the water pump becomes inoperable. Secondly, the accessibility to transport services plays a crucial role in recovery activities. The recovery sequencing algorithm incorporates the availability of the nearest transport node as a necessary condition for scheduling the recovery process.

The industry layer of Shelby County is constructed from the economic census data and the various annual economic surveys conducted by the U.S. Census Bureau. Since the sectoral economic outputs at small geographic levels are not readily available, the following steps are performed to develop the industry layer for the analysis:

1. The county-level data related to total revenue/receipts corresponding to two-digit North American Industry Classification System (NAICS) industry sectors are obtained from the 2017 Annual Business Survey estimates.
2. Zip code-level data on employment size in various two-digit NAICS industries are derived from 2017 County Business Patterns estimates.
3. Assuming that the spatial distribution of annual revenue/receipts follows that of the employment size in different zip code tabulation areas, the zip code-level revenue/receipts are estimated using the proportion of employees in each sector in the corresponding zip code.

Fig. 2(d) shows the total receipts/revenue generated by all industrial sectors in various zip codes in Shelby County.

4.2. Seismic event set and network simulation

The subsequent step to generate ground motion fields for the earthquake scenarios of interest and conduct network simulations to quantify operational and economic losses. Shelby County, situated near the highly active New Madrid Seismic Zone, experiences significant seismic activity, including various point seismic sources in its vicinity. To determine earthquake scenarios suitable for network simulation, a disaggregation analysis is conducted using the 2008 United States National Seismic Hazard Model (Petersen et al., 2008). This analysis focused on assessing seismic hazard at the center of Shelby County, employing a peak ground acceleration (PGA) threshold of $0.5g$, where $g = 9.8\ \mathrm{m/s^2}$. As the present study also emphasizes HILP events, all major seismic rupture scenarios in the region with a probability of exceedance of at least 0.0001 within a return period of 2475 years are considered. The resulting earthquake rupture dataset comprised approximately 250 distinct scenarios, each with an annual occurrence rate ranging from 1E-08 to 1E-02 events per year. Subsequently, event-based simulations are conducted to acquire the ground motion fields. Fig. 3(a) illustrates the peak ground acceleration field of one of the earthquakes in the event set simulated by OpenQuake.

The failure of infrastructure components is modeled using available fragility functions. For this study, the fragility models for determining infrastructure component failures and restoration time distributions based on their robustness are taken from the HAZUS earthquake model technical manual (Federal Emergency Management Agency, 2020). Table A.4 presents the fragility functions and recovery distributions of the various infrastructure components with low level of robustness (see Appendix A.4).

The ground motion fields are mapped to individual infrastructure network components and then applied the relevant fragility curves to derive the damage state probabilities. Since the failure of infrastructure components is modeled probabilistically, three network failure realizations are created for each earthquake scenario under every resilience configuration listed in Table 1. It must be noted that the number of realizations are fixed considering the computational complexity of the simulation model, and a higher number of realizations would provide a more reliable estimate for the network-wide impacts of the seismic events.. Fig. 3(b) illustrates a realization of infrastructure failure resulting from an earthquake of magnitude 7.3 originating in the New Madrid Seismic Zone, located in the northwest of Shelby County.

The infrastructure disruptions and their effects are linked to the industrial layer following a two-step process. First, the magnitude of water and power outages in terms of Equivalent Outage Hours (EOH) in different service areas within Shelby County are computed using InfraRisk. For recovery sequencing, a maximum flow-based component prioritization approach is employed (methodology explained in Balakrishnan and Cassottana (2022)). Fig. 3(c) shows the simulated network performance in terms of satisfied demand percentage resulting from the direct disruptions shown in Fig. 3(b) (see Appendix). Second, the

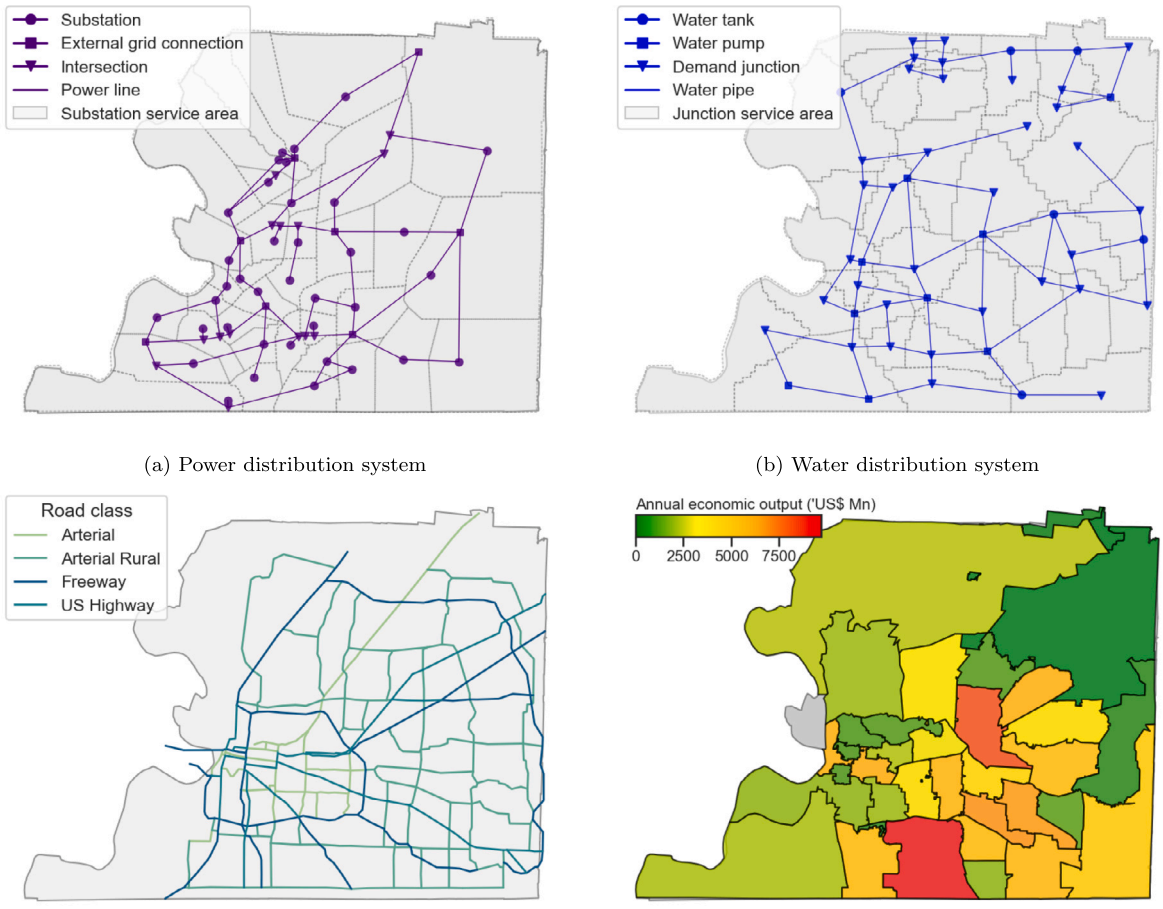

(a) Power distribution system

(b) Water distribution system

(c) Road traffic network

(d) Spatial distribution of aggregate economic output across various zipcodes (industry layer)

Fig. 2. Shelby county interdependent infrastructure network and industry layer.

EOH values corresponding to the service areas are translated to sector-wise disruptions to economic activities and quantified using resilience factors presented by Kajitani and Tatano (2009) using Eq. (3). The resilience factors used in the study are tabulated in Table A.5 (see Appendix A.5). Fig. 3(d) shows the aggregate economic losses incurred by various regions in Shelby County due to the earthquake-induced infrastructure disruptions.

For the present study, a total of 24,000 network simulations are attempted for developing the training dataset (250 earthquake scenarios × 3 infrastructure failure realizations × 8 robustness levels × 4 resourcefulness levels).

4.3. Comparing investment alternatives using Cumulative Prospect Theory

Two types of resilience strategies are considered, aimed at enhancing system robustness (seismic retrofitting or strengthening of components) and resourcefulness (additional post-disaster repair crews and equipment). Table 1 lists the various levels of the two resilience strategies considered.

Seismic retrofitting options (prefixed with 'R') for the integrated power, water, and transport network include converting brittle pipelines to ductile, unanchored tanks and pumping stations to anchored ones, seismic anchoring of substations, gate stations, and towers, and upgrading seismic resistance of roads by better construction. On the other hand, 'C' represents different levels of crew and equipment available for post-disaster recovery. The increased investment in crew and equipment would improve the speed of recovery due to the simultaneous repair and restoration of infrastructure system components. In this study, a 'resilience configuration' is any combination of the two strategies (for example, R1-C1), with R1 and C1 representing the least resilient configurations and R8 and C4 the most resilient ones. The configuration R1-C1 is fixed as the base configuration and analyzed how decision-makers with divergent risk preferences perceive upgrading the infrastructure network to higher resilience configurations. The combination of intermediate resilience configurations represents the pathways through which the highest network resilience level can be achieved. For the unit costs of the infrastructure components, the HAZUS inventory technical manual (Federal Emergency Management Agency, 2021) is largely relied upon (Table 2), and other sources whenever needed. For the post-disaster recovery, we assumed that the annual cost of maintaining a team of repair crew and equipment is equal to 0.25% of the total network replacement value because actual maintenance costs are not available. The crew-level maintenance cost estimates are an approximation based on available network-level maintenance costs and therefore must be treated as assumptions. For each robustness level, a set of fragility curves and recovery functions are defined based on HAZUS-MH guidelines to reflect the improved component robustness.

4.4. Development of optimal pathways for resilience enhancement

Once the network simulations and economic loss analyses are completed, the next step is to calculate the costs and benefits associated

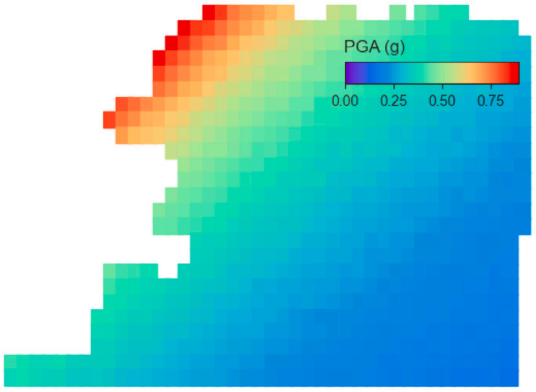

(a) Simulated ground motion field (peak ground acceleration) using OpenQuake

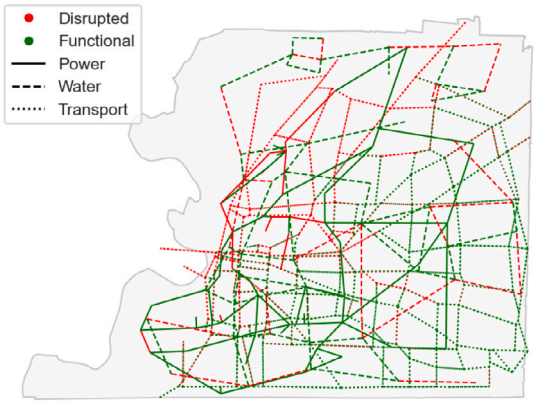

(b) Realization of probabilistic failure of components under the resilience configuration R8-C1 using HAZUS fragility models

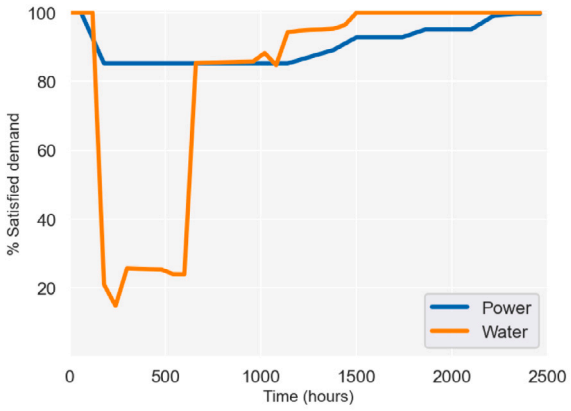

(c) Simulated network recovery curve under the resilience configuration R8-C1 using InfraRisk

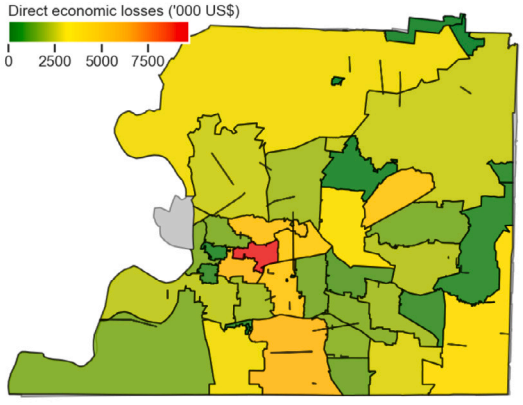

(d) Estimated direct economic costs under the resilience configuration R8-C1

Fig. 3. Simulated infrastructure and business disruptions due to one of the earthquakes from the event set (M = 7.3)

Table 1
Summary of resilience configurations and relevant interventions considered for implementation.

Resilience intervention	Level	Water	Power	Transportation
Robustness	R1	Brittle pipelines, unanchored tanks and pumping stations	Unanchored substations, gate stations and towers	Roads with no seismic resistant design
	R2	Brittle pipelines, unanchored tanks and pumping stations	Anchored substations, gate stations, and towers	Roads with no seismic resistant design
	R3	Ductile pipelines, anchored tanks and pumping stations	Unanchored substations, gate stations and towers	Roads with no seismic resistant design
	R4	Brittle pipelines, unanchored tanks and pumping stations	Unanchored substations, gate stations and towers	Roads with seismic resistant design
	R5	Ductile pipelines, anchored tanks and pumping stations	Anchored substations, gate stations, and towers	Roads with no seismic resistant design
	R6	Brittle pipelines, unanchored tanks and pumping stations	Anchored substations, gate stations, and towers	Roads with seismic resistant design
	R7	Ductile pipelines, anchored tanks and pumping stations	Unanchored substations, gate stations and towers	Roads with seismic resistant design
	R8	Ductile pipelines, anchored tanks and pumping stations	Anchored substations, gate stations, and towers	Roads with seismic resistant design
Resourcefulness	C1	Low level of resourcefulness (10 simultaneous repairs)		
	C2	Moderate level of resourcefulness (20 simultaneous repairs)		
	C3	High level of resourcefulness (30 simultaneous repairs)		
	C4	Very high level of resourcefulness (40 simultaneous repairs)		

with the network resilience configurations as detailed in Section 3.5. For each of the resilience configurations, we calculated the benefits as the annual reduction in physical and economic losses compared to that of the base configuration (R1-C1).

Table 2
Unit costs of infrastructure components.

Component	Unit	Robustness	Replacement cost (US$)
Water tank	each	unanchored	800,000
		anchored	840,000
Water pipeline	meter	brittle	177
		ductile	177
Water pump	each	unanchored	525,000
		anchored	551,250
Power lines and towers	km	unanchored	1,345,514
		anchored	1,364,800
Substation	each	unanchored	10,000,000
		anchored	10,056,000
External grid connection	each	unanchored	100,000,000
		anchored	100,056,000
Road link	km	low seismic resistance	3,334,000
		high seismic resistance	6,668,000

Since the focus is on understanding how decision-makers with varying risk preferences perceive the aforementioned benefits and compare them with upfront costs in the context of high-impact low-probability (HILP) events, four hypothetical decision-makers (DM-A, DM-B, DM-C, and DM-D) are considered. These decision-makers differ in their weighting of low-probability events. To model the risk preferences of the decision-makers, Cumulative Prospect Theory (CPT) is employed, and distinct values are assigned to the γ parameter in the decision weighting function (Eq. (A.7) in Appendix A.1). Specifically, the following four values for γ are examined: 0.2, 0.4, 0.6, and 1.0. These values are selected based on the range of CPT parameter values identified by Reiger et al. (2017) (Rieger, Wang, & Hens, 2017) through an international survey. $\gamma = 0.2$ represents a decision-maker who assigns *very high* weights to low-probability events (DM-A), while $\gamma = 1.0$ represents a *neutral* and rational decision-maker (DM-D). The weighting parameter values $\gamma = 0.4$ and $\gamma = 0.6$ correspond to decision-makers with *high* and *moderate* preferences towards low-probability events, respectively (DM-B and DM-C). For simplicity, $\alpha = 1$ is assumed for transforming benefits using the value function of CPT (Eq. (A.3) in Appendix A.1).

Major resilience projects are typically implemented over several years. Given a certain amount of investment, there are an infinite number of ways to allocate resources to various resilience strategies. To identify optimal resilience pathways within the Shelby County infrastructure network, the resource allocation optimization problem presented in Eq. (20) is solved. Throughout the study, we assumed the following values for the model parameters, unless otherwise specified: an investment horizon (T_I) of 15 years, a design horizon (T_D) of 50 years, a planned aggregate budget ($\mathbb{C}$) of $100 million, and a discount rate (r) of 2%. Linear regression models are developed to predict the prospects of infrastructure resilience upgrades, as perceived by the four decision-makers based on the allocation amounts for each intervention. Table 3 summarizes a subset of the regression models developed for the four decision-makers (corresponding to a total budget of $100 million, a model exponent of 1.0, and a discount rate of 2.0%). The model coefficients (β_{n_i}) indicate the change in prospects for every dollar spent on the respective resilience intervention, with other variables held constant. For instance, DM-A (who assigns a *very high* degree of overweighting for low probability events) perceives a return of $4.237 for every dollar invested in improving water network robustness when using a model exponent value of one. Conversely, DM-D (who assigns neutral weights to probabilities) estimates the return on one dollar invested in improving water network robustness to be only $0.0016. Similar models are also built for the decision-makers under different model exponents, cumulative budgets and discount rates considered in the study.

The regression models are applied to the resource allocation optimization problem, which computes the percentage of annual investment allocated to the four interventions throughout the investment horizon. Fig. 4 illustrates the optimal resilience pathway according to the risk preferences of DM-B (who has a *high* degree of overweighting for the low-probability events, $\gamma = 0.4$), assuming a total budget of $100 million, a model exponent value of 1.1, and a discount rate of 2%. Fig. 4(a) shows the annual budget share during the investment horizon and Fig. 4(b) shows the percentage of each network for which the specific intervention is implemented. The dotted vertical line represents the threshold year (calculated using Eq. (21)) beyond which the decision-maker perceives further investments as infeasible due to the total upgrade costs exceeding the perceived gains (hatched region). The annual budget share values within the hatched region in Fig. 4(a) indicate the resource allocation scheme if feasibility of investments are not taken into consideration. The results reveal that within the feasible region, the largest share of the investment is allocated to adding more crew and equipment, followed by investments in water network robustness and power network robustness.

Fig. 4(b) reveals that investments in power network robustness are the most preferred in terms of cost-effectiveness, followed by crew and equipment and water network robustness. No significant funds are allocated, both in the feasible and infeasible regions, for improving transportation robustness, primarily due to its high upfront costs. Moreover, the highly interconnected nature of the Shelby transportation network may mitigate the need for reinforcing existing road links, as the accessibility to different nodes may not be significantly affected even in the event of multiple road link disruptions caused by earthquakes.

4.5. Effect of risk preferences of decision-makers and budget on the resilience pathways

Fig. 5 shows the combined sensitivity of the resource allocation scheme against the risk preference of the decision-makers and the total budget allocated over the investment horizon. Each row of Fig. 5 represents how decision-makers with varied risk preferences, i.e. weighting, for low-probability events perceive the loss reduction from investing in resilience interventions and decide on them. Each column illustrates how decision-makers with a certain risk preference allocate resources to different interventions based on different aggregate budgets. Significant differences in resource allocation schemes appear among decision-makers with different risk perceptions. Namely, with a fixed budget of $100 million, DM-D (who assigns *neutral* weights to low-probability events) allocates the majority of the initial years to water network robustness, followed by power robustness. Conversely, DM-A (who attributes *very high* weights to low-probability events) prioritizes crew and equipment and power robustness. There is a clear shift from a preference for investing in water robustness to investing in crew and equipment as decision-makers increase their weights on low-probability events. This trend suggests that investing in post-disaster recovery is preferred by decision-makers as an effective way to address resilience against HILP events compared to investing in reinforcing the infrastructure components to strengthen them against large seismic shocks. Remarkably, improving power robustness is highly preferred by all decision-makers owing to its low upfront costs and high prospects. Regarding feasibility, it is evident that decision-makers with neutral or near-neutral risk preferences (DM-C and DM-D) do not consider the resilience interventions feasible, even during the initial years of the investment horizon. However, those who assign higher weights to low-probability events (DM-A and DM-B) perceive that even large investments in resilience are worthwhile when considering their capability to reduce losses against HILP events.

In addition to the analysis mentioned above, we developed characteristic curves for each decision-maker. These curves illustrate the

Table 3
Summary of regression models to predict prospects of resilience investments (budget = $200Mn, model exponent = 1.0, and discount rate = 2%).

Decision maker	γ	ξ	β_w (t-stat)	β_p (t-stat)	β_t (t-stat)	β_r (t-stat)	F-statistic	Adj. R^2
DM-A	0.2	1	4.27 (3.570)	69.33 (7.789)	0.39 (9.502)	6.39 (8.458)	247.85	0.97
DM-B	0.4	1	0.41 (5.130)	3.25 (5.521)	0.02 (10.626)	0.40 (8.165)	249.002	0.97
DM-C	0.6	1	0.05 (6.512)	0.19 (3.226)	0.003 (9.524)	0.04 (7.895)	213.616	0.965
DM-D	1.0	1	0.002 (7.451)	0.003 (1.662)	0.001 (6.407)	0.001 (7.714)	159.785	0.953

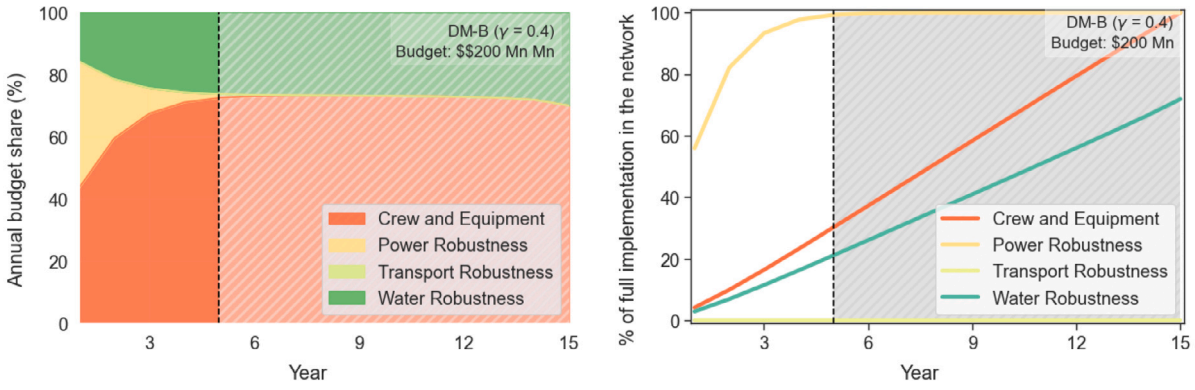

(a) Annual budget share (%) (b) Percentage of network covered

Fig. 4. Optimal budget allocation over the investment horizon for Shelby County infrastructure network (Decision-maker: DM-B (γ = 0.4), budget: $200 Mn, model exponent: 1.1, and discount rate: 2%). The hatched region represents the infeasible region as perceived by the decision-maker.

relationship between the total investment in resilience and the corresponding perceived gains based on the optimization results. Fig. A.8 (refer to Appendix A.6) demonstrates how the perceived gains vary for different decision-makers as resilience investments increase. The figure also indicates the thresholds at which decision-makers consider further investments to be infeasible.

4.6. Effect of discount rates and model exponent on resource allocation

Similar to the influence of budget and decision-maker risk preferences on resource allocation, the effect of discount rates and model exponents are also investigated. Discount rates r determine the net present value (NPV) of annual allocations during the investment period, while the model exponent determines the rate of change in marginal returns from investments. Four discount rates for the analysis are considered (0%, 2%, 5%, and 10%). As expected, higher discount rates reduce the NPV of resilience investments and, consequently, decrease the marginal returns. Therefore, the feasible investment region is reduced, and the threshold year shifts to the left when a higher discount rate is considered (Fig. 6). For example, when a total budget of $100 million is allocated by DM-B, the threshold for feasible investment corresponding to a discount rate of 2% is 11 years (equivalent to an investment of (100 million/15) × 5 = $73.33 million). In contrast, the corresponding threshold is 8 years when the discount rate is 10% (equivalent to $53.33 million). However, it is important to note that the annual budget allocation schemes are not significantly affected by the discount rates.

The selection of the model exponent ξ also has a considerable effect on the resource allocation schemes. We considered four values for model exponent: 1.0, 1.1, 1.5, and 2.0. The results show that, for a fixed budget and discount rate, the variation in the budget share for various interventions is reduced. Fig. 7 illustrates the resource allocation schemes by DM-B when the budget is fixed at $100 million and the discount rate is 2%. When a model exponent of 1 is used, the standard deviation in the annual budget share for the first year is 50%, whereas when a model exponent of 1.5 is used, the standard deviation for the same is 21%. These trends hold true throughout the investment period. One possible reason is that having a higher model exponent (which implies diminishing marginal returns for the resilience interventions) makes all interventions relatively attractive to decision-makers, regardless of their risk preferences.

It is also worthwhile to note the effect of the model exponent on the length of feasibility regions. Mathematically, a higher model exponent value denotes higher marginal returns per dollar spent for the initial investments, resulting in a higher investment threshold for costs to exceed the perceived gains. Higher exponent values in the model can be a result of highly optimized and targeted resource allocation schemes within a specific infrastructure network. The feasibility regions under various values of mode exponents suggest that identifying the components within infrastructure systems that can have considerable effect on reducing annual losses may help in convincing even *neutral* decision-makers to invest in resilience.

5. Conclusions

In this study, we presented a methodology for developing optimal resilience pathways for interdependent infrastructure networks. Instead of the traditional 'silo' approach commonly used by infrastructure agencies, a system-of-systems perspective is adopted, considering power, water, and transport systems as interconnected entities. The study analyzed how these systems collectively respond to catastrophic earthquakes and incorporated the resulting business disruptions into a resilience decision-making framework. By combining an infrastructure-industry simulation framework with Cumulative Prospect Theory, the study also explored the influence of decision-makers' risk preferences on infrastructure resilience resource allocation.

Based on experimental simulations on the Shelby County infrastructure network, the study demonstrated that certain decision-makers (specifically those who overweight low probabilities) perceive resilience interventions aimed at mitigating HILP events as more cost-effective and appealing compared to risk-neutral decision-makers. The resilience investment problem is formulated in a manner analogous to lotteries, where individuals make a payment with the expectation of a much larger return, even if the probability of achieving that outcome is very low. Upgrading the resilience of infrastructure systems also involves significant resource expenditure in anticipation of reduced cumulative

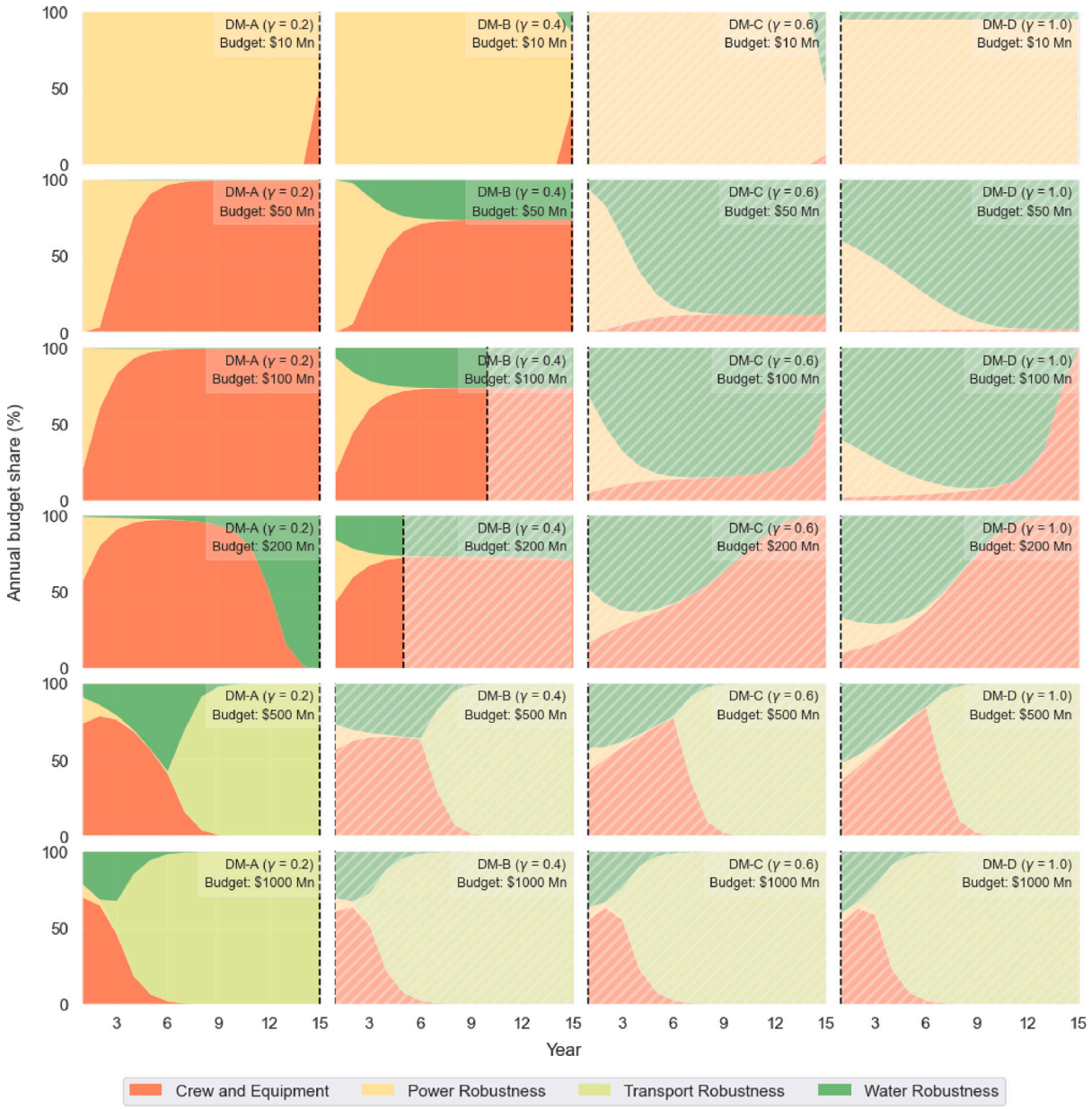

Fig. 5. Sensitivity analysis for budget and probability weighting (discount rate: 2%, model exponent: 1.1). The hatched region represents the infeasible region as perceived by the decision-maker.

losses when HILP events occur. The variations in risk perceptions among decision-makers towards low probabilities lead to different budget allocations and, consequently, divergent resilience upgrade pathways. As expected, the decision-makers who assign higher weights to low-probability events (even if agnostic to the consequences of those events) tend to allocate more resources for resilience enhancement compared to risk-neutral decision-makers. More interestingly, it was also revealed that resource allocation by such decision-makers often prioritizes post-disaster recovery measures over pre-disaster robustness alternatives, resulting in a trade-off when investing in resilience for HILP events compared to risk-neutral cost–benefit analysis (CBA) approaches. In addition, the analysis of the resource allocation schemes revealed that efforts to maximize the marginal returns from resilience investments in individual infrastructure systems can lead to higher investment thresholds by decision-makers. This can be achieved through prioritized and targeted resource allocation to critical components within the infrastructure systems. On the other hand, the sensitivity analysis also showed that the identified resource allocation schemes are less sensitive to discount rates across all decision-makers.

The study made two distinct contributions to the literature. Firstly, it considered infrastructure systems as a system-of-systems with socioeconomic obligations to evaluate resilience upgrade alternatives. Secondly, it investigated the influence of decision-maker risk preferences (specifically their perception of low-probability events) in infrastructure resilience planning outcomes, providing useful insights on how certain decision-makers may allocate more resources towards resilience enhancement compared to risk-neutral decision-makers. While the proposed methodology is developed in the context of seismic risks, it can also be extended to other hazards and multi-hazards to develop cost-effective resilience pathways for interdependent infrastructure systems.

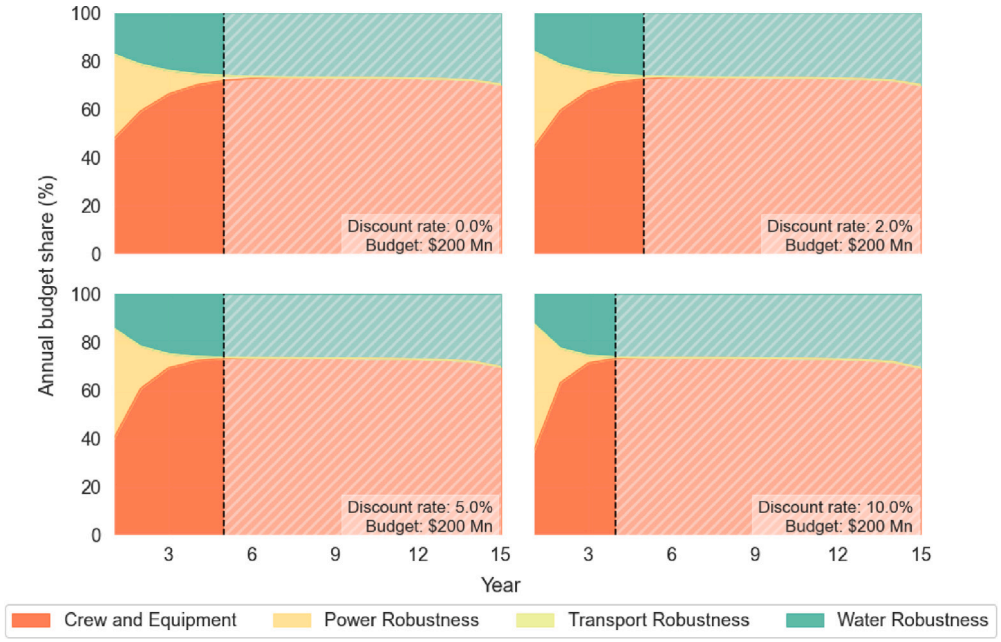

Fig. 6. Sensitivity analysis for discount rates (Decision-maker: DM-B (γ = 0.4), budget: $200 Mn, model exponent = 1.1). The hatched region represents the infeasible region as perceived by the decision-maker.

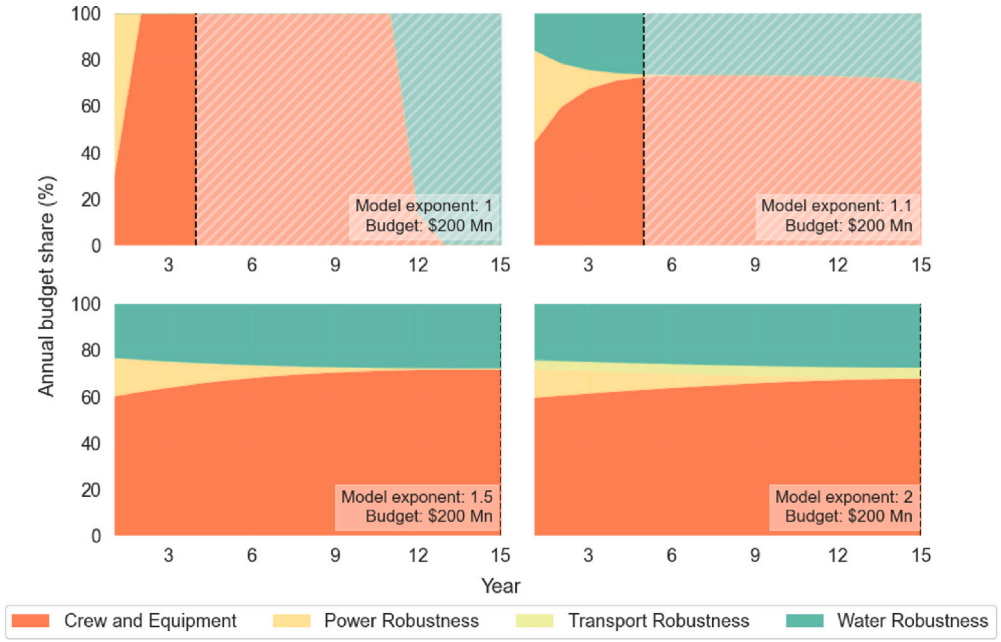

Fig. 7. Sensitivity analysis for model exponents (Decision-maker: DM-B (γ = 0.4), budget: $200 Mn, discount rate: 2%). The hatched region represents the infeasible region as perceived by the decision-maker.

CRediT authorship contribution statement

Srijith Balakrishnan: Writing – review & editing, Writing – original draft, Visualization, Validation, Supervision, Software, Project administration, Methodology, Investigation, Formal analysis, Data curation, Conceptualization. **Lawrence Jin:** Writing – review & editing, Validation, Methodology, Investigation, Conceptualization. **Beatrice Cassottana:** Writing – review & editing, Validation, Supervision, Methodology, Funding acquisition, Conceptualization. **Alberto Costa:** Writing – review & editing, Validation, Methodology. **Giovanni Sansavini:** Writing – review & editing, Validation, Supervision, Resources, Methodology, Conceptualization.

Declaration of competing interest

The authors declare the following financial interests/personal relationships which may be considered as potential competing interests: Beatrice Cassotana reports financial support was provided by Prime Minister's Office Singapore. If there are other authors, they declare that they have no known competing financial interests or personal relationships that could have appeared to influence the work reported in this paper.

Data availability

The *InfraRisk* package can be downloaded from GitHub[2]. Documentation and codes for sample simulations are available in the *InfraRisk* package. The final processed datasets and analysis codes of this study are available on 4TU.ResearchData repository[3].

Acknowledgments

This research is supported by the National Research Foundation, Prime Minister's Office, Singapore under its Campus for Research Excellence and Technological Enterprise (CREATE) programme.

Appendix. Supporting descriptions and data

A.1. Frameworks to incorporate risk preferences in decision-making

This subsection provides a brief overview of Expected Utility Theory (EUT) and Cumulative Prospect Theory (CPT).

A.1.1. Expected Utility Theory

Expected Utility Theory (EUT) is a fundamental theory in decision theory and economics that provides a framework for decision-making under uncertainty. EUT assumes that decision-makers evaluate outcomes based on their expected utilities, which are calculated by weighting the utilities of different outcomes by their respective probabilities.

In EUT, decision-makers are assumed to be rational and make choices that maximize their expected utility. The utility function represents the decision-maker's preferences, indicating how they value different outcomes. The utility function is typically assumed to be increasing and concave, reflecting diminishing marginal utility of gains. A commonly used form of the utility function is the power utility function, given by Eq. (A.1).

$$u(x) = \frac{x^{(1-\rho)}}{1-\rho} \tag{A.1}$$

where u represents the utility function, x represents the outcome, and ρ represents the coefficient of risk-aversion. A higher value of ρ indicates higher risk-aversion.

To evaluate decision alternatives under uncertainty using EUT, decision-makers calculate the expected utility of each alternative. The expected utility is determined by taking a weighted average of the utilities of the possible outcomes, where the weights are given by the probabilities of those outcomes. Mathematically, the expected utility denoted as EU, is calculated as shown in Eq. (A.2):

$$EU = \sum_{i=1}^{n} p_i u(x_i) \tag{A.2}$$

where p_i represents the probability of outcome i, x_i represents the value of outcome i, and n represents the total number of possible outcomes.

Expected Utility Theory provides a normative framework for decision-making under uncertainty, assuming that decision-makers are rational and consistent in their preferences.

A.1.2. Cumulative Prospect Theory

Cumulative Prospect Theory (CPT) is an extension of the EUT proposed by Tversky and Kahneman (1992) to describe how decision-makers perceive and evaluate consequences and make decisions under uncertainty. The subjective factors influencing the irrational behavior of decision-makers who evaluate outcomes of events are captured using two components, namely a value function and the probability weighting function.

The value function defines how individuals perceive gains and losses. The value function is concave for gains, indicating that decision-makers have decreasing sensitivity to higher gains, whereas it is convex for losses, suggesting increasing sensitivity to losses. Therefore, decision-makers tend to be risk-averse over gains, whereas they are risk-seeking about losses. The commonly adopted utility function in CPT is presented in Eq. (A.3):

$$\upsilon(x) = \begin{cases} x^{\alpha} & x \geq 0 \\ -\lambda(-x)^{\beta} & x < 0 \end{cases} \tag{A.3}$$

where υ is the value function, x is the gain (or loss), λ is the loss-aversion coefficient, and α and β describe the risk attitudes for gains and losses. In the current study, we are evaluating the reduction in potential losses due to physical and economic disruptions by investing in resilience alternatives. Therefore, we focus solely on gains in the decision-making process.

The second part is the probability weighting function, which explains how individuals distort probabilities when assessing risks. CPT suggests that decision-makers tend to assign larger weights to low probabilities, while higher probabilities are underweighted. This feature makes CPT an attractive framework for studying how decision-makers perceive HILP events and the resulting divergence in decisions regarding resource allocation. According to CPT, if the outcomes of an experiment, along with their corresponding probabilities, are represented as $(x_1, P_1; x_2, P_2; \ldots; x_n, P_n)$ and if $x_1 \leq \cdots \leq 0 \leq x_{k+1} \leq \cdots \leq x_n$, then the CPT values of prospect are given by Eq. (A.4).

$$G = \sum_{i=1}^{k} \pi_i^- \upsilon(x_i) + \sum_{i=k+1}^{n} \pi_i^+ \upsilon(x_i) \tag{A.4}$$

where the decision weights π_i^- and π_i^+ are defined as:

$$\pi_1^- = w^-(P_1); \quad \pi_i = w^-(P_1 + P_2 \cdots + P_i) - w^-(P_1 + P_2 \cdots + P_{i-1}) \quad 1 < i \leq k \tag{A.5}$$

$$\pi_n^+ = w^+(P_n); \quad \pi_i = w^+(P_i + \cdots + P_n) - w^+(P_{i+1} + \cdots + P_n) \quad k+1 \leq i < n \tag{A.6}$$

The decision weighing function is given by Eq. (A.7).

$$w^{\pm}(P) = \frac{P^{\gamma}}{(P^{\gamma} + (1-P)^{\gamma})^{\frac{1}{\gamma}}} \tag{A.7}$$

[2] https://github.com/srijithbalakrishnan/dreaminsg-integrated-model.

[3] Balakrishnan, S. (2023), Cost–benefit analysis of infrastructure resilience investments: Shelby County, 4TU.ResearchData.

where P is the probability value and $\gamma \in [0, 1]$ is the amount of over or under weighting.

A.2. Steps to develop the seismic event set and corresponding ground motion fields

The following steps outline the process for selecting the final earthquake scenarios for infrastructure simulations.

1. To select the earthquake rupture events based on probability of exceedance (P_e), an investigation period T is chosen.
2. A ground motion parameter value of interest is selected, and a disaggregation analysis of the seismic hazard within the region is conducted. In OpenQuake, direct disaggregation of the seismic hazard by source and magnitude is not possible. Therefore, the hazard is initially disaggregated at the center of the study region by source to determine the probability of exceedance for each source ($P(X \geq x|T, \ell)$, where X represents the ground motion value, x denotes the threshold for the ground motion parameter, T represents the investigation period, and ℓ is the seismic source). The sources that surpass the above predefined threshold for the probability of exceedance are identified. The percentage contribution of each source to the seismic hazard is then calculated according to Eq. (A.8) as in Pagani, Monelli, Weatherill, and Garcia (2014).

$$\mathcal{P}_{\ell} = \frac{-\ln(1 - P(X \geq x|T, \ell))}{-\ln\left(1 - \prod_{\ell \in L} P(X \geq x|T, \ell)\right)} \times 100 \tag{A.8}$$

   Next, each source is selected and disaggregation analysis of its hazard contribution by magnitude is performed. This allowed us to obtain the conditional probability of exceedance for each source by magnitude ($P(X \geq x|T, \ell, M)$, where M represents the magnitude). Similar to Eq. (A.8), the conditional percentage of contribution $\mathcal{P}_{M|\ell}$ is calculated based on the probability of exceedance values. Subsequently, the contribution of a seismic rupture originating from seismic source ℓ with magnitude M is also calculated using Eq. (A.9).

$$\mathcal{P}_{M,\ell} = \frac{\mathcal{P}_{\ell}}{100} \times \mathcal{P}_{M|\ell} \tag{A.9}$$

3. Having identified the seismic ruptures, the subsequent step involved simulating the ground motion fields associated with each of the selected rupture scenarios. To accomplish this, the boundaries of the study region are defined, and equidistant points are established at which various ground motion parameters, such as peak ground acceleration (PGA), peak ground velocity (PGV), and peak ground displacement (PGD), are to be evaluated. Subsequently, event-based seismic simulations are performed in OpenQuake for the chosen geographical points.

A.3. Interdependent infrastructure simulation: Main modules of InfraRisk model

In this section, the various modules within the InfraRisk simulation model is briefly detailed. For a more elaborate reading, readers are suggested to refer to the original paper (Balakrishnan & Cassottana, 2022). InfraRisk comprises of five distinct modules as follows:

1. Integrated infrastructure network simulation: This module focuses on simulating the behavior and interactions of the interconnected infrastructure components within the network. InfraRisk can simulate the interdependent effects of water-, power-, and transport networks. It uses Python packages, namely *wntr* for water networks (Klise et al., 2020), *pandapower* for power networks (Thurner et al., 2018), and a Python implementation of the static traffic assignment model f or transport networks (Boyles, Lownes, & Unnikrishnan, 2020). The module also considers major dependencies among these three infrastructure systems to allow for cascading failures.
2. Hazard initiation and vulnerability modeling: This module handles the modeling of hazards and the vulnerability of infrastructure components to these hazards. It can also be coupled with hazard models, such as OpenQuake, to induce infrastructure component failures prior to network simulation.
3. Recovery modeling: The recovery modeling module simulates the post-disruption recovery process of the infrastructure components, considering factors such as repair time and resource availability. Topological characteristics, such as centrality measures, and operational characteristics, such as maximum daily flow rate, are used to derive recovery sequences and schedules in the model.
4. Simulation of direct and indirect effects: This module captures both direct and indirect effects of infrastructure disruptions, considering the interdependencies within the infrastructure network. The integrated infrastructure simulation is carried out in two steps: event table generation and interdependent infrastructure simulation. The event table serves as a reference for scheduling disruptions and repair actions required for the interdependent network simulation. Once the event table is created, the interdependent effects resulting from component disruptions and subsequent restoration efforts are simulated.
5. Resilience quantification: The resilience quantification module assesses the overall resilience of the integrated infrastructure network by analyzing various indicators and metrics. The metrics capture the satisfied demand (ratio of supply to demand) of different infrastructure services at the respective demand nodes. The water and power disruptions at the demand nodes are quantified in terms of the Equivalent Outage Hours (hours) and are denoted by EOH_w and EOH_p, respectively.

A.4. HAZUS fragility- and recovery model parameters of infrastructure components considered in the study

See Table A.4.

A.5. Inoperability factors for linking infrastructure service disruptions with economic losses

See Table A.5.

A.6. Characterizing the resilience investment thresholds for different decision-makers

Fig. A.8 characterizes the relationship between resilience investment costs and perceived gains in reducing physical and economic costs from disasters for decision-makers with varying risk preferences. The color-coded lines represent the decision-makers with different levels of probability weighting. The dashed line represents the break-even line on which the total resilience costs equal perceived gains. The hatched region on the graph indicates that decision-makers, based on their risk preferences, may find that the costs of additional resilience measures outweigh the perceived gains in reducing physical and economic costs from disasters.

The characteristic lines representing the four decision-makers on are plotted based on the resource allocation solutions obtained from the optimization problem discussed in Eq. (20). It can be observed that decision-makers with higher weights for low-probability events (DM-A followed by DM-B) are willing to spend higher amounts on resilience. However, for the Shelby County case study, decision-makers DM-C and DM-D, who have relatively lower weights for low probabilities, do not perceive any feasible gains from resilience investments.

Table A.4
Fragility functions and recovery time distributions of infrastructure components with low level of robustness.
Source: HAZUS manuals.

System	Component	Fragility model				Recovery model		
		d	IM[a]	θ_d	Φ_d	μ_R (days)	σ_R (days)	v^d
Water	Water pump (unanchored)	Slight	PGA	0.13	0.6	0.9	0.3	0.05
		Moderate		0.28	0.5	3.1	2.7	0.38
		Extensive		0.77	0.65	5	3	0.8
		Complete		1.5	0.8	10	3	1
	Water tank (unanchored)	Slight	PGA	0.15	0.6	1.2	0.4	0.2
		Moderate		0.4	0.6	3.1	2.7	0.4
		Extensive		0.7	0.7	93	85	0.8
	Water pipeline (brittle)	Moderate	RR	0.1	1.5	0.3	0	0.3
		Extensive		0.5	1.5	0.3	0	0.8
Power	Substation (unanchored)	Slight	PGA	0.1	0.6	1	0.5	0.05
		Moderate		0.2	0.5	3	1.5	0.11
		Extensive		0.3	0.4	7	3.5	0.55
		Complete		0.5	0.4	30	15	1
	External grid connection (unanchored)	Slight	PGA	0.09	0.5	1	0.5	0.05
		Moderate		0.13	0.4	3	1.5	0.11
		Extensive		0.17	0.35	7	3.5	0.55
		Complete		0.38	0.35	30	15	1
	Power line (unanchored)	Slight	PGA	0.24	0.25	0.3	0.2	0.05
		Moderate		0.33	0.2	1	0.5	0.15
		Extensive		0.58	0.15	3	1.5	0.6
		Complete		0.89	0.15	7	3	1
	Switch (unanchored)	Slight	PGA	0.24	0.25	0.3	0.2	0.05
		Moderate		0.33	0.2	1	0.5	0.15
		Extensive		0.58	0.15	3	1.5	0.6
		Complete		0.89	0.15	7	3	1
Transport	Road link (low seismic resistance)	Slight	PGD	6	0.7	0.4	0	0.05
		Moderate		12	0.7	1.1	0.45	0.2
		Extensive		24	0.7	10.5	4	0.7

[a] The intensity measures (IM) include peak ground acceleration (PGA in g), peak ground velocity (PGV in cm/s), peak ground displacement (PGD in $inches$), and recovery rate (RR in repairs per km) .

Table A.5
Inoperability values of economic sectors calculated from resilience factors presented by Kajitani and Tatano (2009).

Industry	NAICS	η_p	η_w	η_{pw}
Agriculture, Forestry, Fishing and Hunting	11	0.75	0.29	0.75
Mining, Quarrying, and Oil and Gas Extraction	21	0.25	1	1
Utilities	22	0.95	0.45	0.97
Construction	23	0.71	0.31	0.77
Manufacturing	31–33	0.95	0.45	0.97
Wholesale Trade	42	0.79	0.42	0.8
Retail Trade	44–45	0.79	0.42	0.8
Transportation and Warehousing	48–49	0.73	0.23	0.79
Information	51	0.75	0.16	0.81
Finance and Insurance	52	0.59	0.2	0.69
Real Estate and Rental and Leasing	53	0.56	0.4	0.6
Professional, Scientific, and Technical Services	54	0.74	0.22	0.82
Management of Companies and Enterprises	55	0.74	0.22	0.82
Administrative and Support and Waste Management and Remediation Services	56	0.74	0.22	0.82
Educational Services	61	0.74	0.22	0.82
Health Care and Social Assistance	62	0.68	0.48	0.81
Arts, Entertainment, and Recreation	71	0.75	0.25	0.75
Accommodation and Food Services	72	0.8	0.5	0.85
Other Services (except Public Administration)	81	0.74	0.22	0.82
Public Administration	92	0.75	0.25	0.75

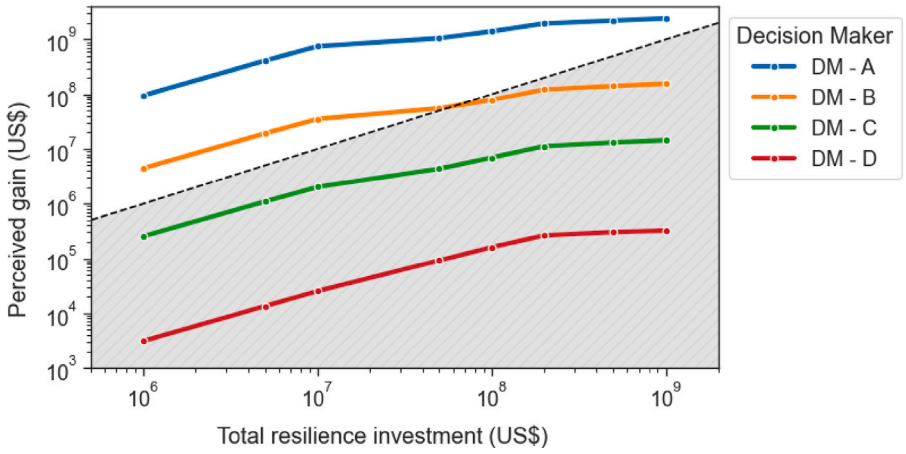

Fig. A.8. Characteristic curves showing the relationship between total resilience investments and perceived gain by different stakeholders (discount rate: 2%, model exponent: 1.1; dashed line represent break-even line; hatched region represent infeasible investment).

References

Altman, M. (2010). Prospect theory and behavioral finance. *Behavioral Finance: Investors, Corporations, and Markets*, 191–209.

Balakrishnan, S., & Cassottana, B. (2022). InfraRisk: An open-source simulation platform for resilience analysis in interconnected power–water–transport networks. *Sustainable Cities and Society*, *83*, Article 103963. http://dx.doi.org/10.1016/j.scs.2022.103963.

Barberis, N. C. (2013). Thirty years of prospect theory in economics: A review and assessment. *Journal of Economic Perspectives*, *27*(1), 173–196.

Béné, C., Wood, R. G., Newsham, A., & Davies, M. (2012). Resilience: New utopia or new tyranny? Reflection about the potentials and limits of the concept of resilience in relation to vulnerability reduction programmes. *IDS Working Papers*, *2012*, 1–61. http://dx.doi.org/10.1111/J.2040-0209.2012.00405.X.

Boyles, S. D., Lownes, N. E., & Unnikrishnan, A. (2020). Transportation network analysis, *vol. 1*, (0.85 ed.).

Bruneau, M., Chang, S. E., Eguchi, R. T., Lee, G. C., O'Rourke, T. D., Reinhorn, A. M., et al. (2003). A framework to quantitatively assess and enhance the seismic resilience of communities. *Earthquake Spectra*, *19*, 733–752. http://dx.doi.org/10.1193/1.1623497.

Carlson, J., Haffenden, R., Bassett, G., Buehring, W., Collins, M., III, Folga, S., et al. (2012). *Resilience: Theory and Application*. http://dx.doi.org/10.2172/1044521.

Cha, E. J., & Ellingwood, B. R. (2012). Risk-averse decision-making for civil infrastructure exposed to low-probability, high-consequence events. *Reliability Engineering & System Safety*, *104*, 27–35. http://dx.doi.org/10.1016/J.RESS.2012.04.002.

Chadburn, O., Jacobo, O., Kenst, K., & Venton, C. C. (2010). *Cost benefit analysis for community based climate and disaster risk management: synthesis report*: *Tech. rep.*, Commissioned by Tearfund and Oxfam America, URL https://www.preventionweb.net/files/14851_FinalCBASynthesisReportAugust2010.pdf. (Accessed 20 October 2023).

Chang, S. E. (2016). Socioeconomic impacts of infrastructure disruptions. In *Oxford Research Encyclopedia of Natural Hazard Science*. Oxford University Press, http://dx.doi.org/10.1093/ACREFORE/9780199389407.013.66.

Chang, S. E., Seligson, H. A., & Eguchi, R. T. (1996). *Estimation of the economic impact of multiple lifeline disruption: Memphis light, gas and water division case study*: *Tech. rep.*, Buffallo, New York: National Center for Earthquake Engineering and Research, State University of New York at Buffallo.

Cheng, M., & Frangopol, D. M. (2022). Life-cycle optimization of structural systems based on cumulative prospect theory: Effects of the reference point and risk attitudes. *Reliability engineering and system safety*, *218*, Article 108100.

Chi, S., & Bunker, J. (2021). An Australian perspective on real-life cost-benefit analysis and assessment frameworks for transport infrastructure investments. *Research in Transportation Economics*, *88*, Article 100946. http://dx.doi.org/10.1016/J.RETREC.2020.100946.

Croope, S. V., & McNeil, S. (2011). Improving resilience of critical infrastructure systems postdisaster: Recovery and mitigation. *Transportation Research Record: Journal of the Transportation Research Board*, *2234*, 3–13. http://dx.doi.org/10.3141/2234-01.

Esmalian, A., Yuan, F., Rajput, A. A., Farahmand, H., Dong, S., Li, Q., et al. (2022). Operationalizing resilience practices in transportation infrastructure planning and project development. *Transportation Research Part D: Transport and Environment*, *104*, Article 103214. http://dx.doi.org/10.1016/J.TRD.2022.103214.

Federal Emergency Management Agency (2020). *Hazus Earthquake Model Technical Manual: Hazus 4.2 SP3*: *Tech. rep*, Washington D.C.: United States Department of Homeland Security, URL www.fema.gov/sites/default/files/2020-10/fema_hazus_earthquake_technical_manual_4-2.pdf. (Accessed 10 October 2023).

Federal Emergency Management Agency (2021). *Hazus inventory technical manual hazus 4.2 service pack 3*: *Tech. rep.*, Washington D.C.: United States Department of Homeland Security, URL www.fema.gov/sites/default/files/2020-10/fema_hazus_earthquake_technical_manual_4-2.pdf. (Accessed 10 October 2023).

Francis, R., & Bekera, B. (2014). A metric and frameworks for resilience analysis of engineered and infrastructure systems. *Reliability Engineering & System Safety*, *121*, 90–103. http://dx.doi.org/10.1016/J.RESS.2013.07.004.

Gayer, G. (2010). Perception of probabilities in situations of risk: A case based approach. *Games and Economic Behavior*, *68*, 130–143. http://dx.doi.org/10.1016/J.GEB.2009.05.002.

Gharaibeh, N. G., Chiu, Y.-C., & Gurian, P. L. (2006). Decision methodology for allocating funds across transportation infrastructure assets. *Journal of Infrastructure Systems*, *12*, 1–9. http://dx.doi.org/10.1061/(ASCE)1076-0342(2006)12:1(1).

Güneralp, B., Güneralp, I., & Liu, Y. (2015). Changing global patterns of urban exposure to flood and drought hazards. *Global Environmental Change*, *31*, 217–225. http://dx.doi.org/10.1016/J.GLOENVCHA.2015.01.002.

Haimes, Y. Y., Horowitz, B. M., Lambert, J. H., Santos, J. R., Lian, C., & Crowther, K. G. (2005). Inoperability input-output model for interdependent infrastructure sectors. I: Theory and methodology. *Journal of Infrastructure Systems*, *11*(2), 67–79. http://dx.doi.org/10.1061/(ASCE)1076-0342(2005)11:2(80).

Hallegatte, S., Rentschler, J., & Rozenberg, J. (2019). *Lifelines: The resilient infrastructure opportunity*. Washington, DC: World Bank, http://dx.doi.org/10.1596/978-1-4648-1430-3.

Hallegatte, S., Rozenberg, J., Rentschler, J., Nicolas, C., & Fox, C. (2019). *Strengthening new infrastructure assets: A cost-benefit analysis*. The World Bank, http://dx.doi.org/10.1596/1813-9450-8896, URL https://elibrary.worldbank.org/doi/abs/10.1596/1813-9450-8896.

IBM ILOG (2015). *IBM ILOG CPLEX 12.6 User's Manual*. Gentilly, France: IBM ILOG, cplex126 URL https://public.dhe.ibm.com/software/products/Decision_Optimization/docs/pdf/usrcplex.pdf.

Jones, H., Moura, F., & Domingos, T. (2014). Transport infrastructure project evaluation using cost-benefit analysis. *Procedia - Social and Behavioral Sciences*, *111*, 400–409. http://dx.doi.org/10.1016/J.SBSPRO.2014.01.073.

Kahneman, D., & Tversky, A. (1979). Prospect theory: An analysis of decision under risk. *Econometrica*, *47*(2), 263–292.

Kajitani, Y., & Tatano, H. (2009). Estimation of lifeline resilience factors based on surveys of Japanese industries. *Earthquake Spectra*, *25*, 755–776. http://dx.doi.org/10.1193/1.3240354.

Klise, K., Hart, D., Bynum, M., Hogge, J., Haxton, T., Murray, R., et al. (2020). *Water network tool for resilience (WNTR) user manual*: *Tech. rep.*, Albuquerque, NM (United States): Sandia National Lab.(SNL-NM).

Li, Y., Su, S., Liu, B., Yamashita, K., Li, Y., & Du, L. (2022). Trajectory-driven planning of electric taxi charging stations based on cumulative prospect theory. *Sustainable Cities and Society*, *86*, Article 104125.

Manyena, B., Machingura, F., & O'Keefe, P. (2019). Disaster Resilience Integrated Framework for Transformation (DRIFT): A new approach to theorising and operationalising resilience. *World Development*, *123*, Article 104587. http://dx.doi.org/10.1016/J.WORLDDEV.2019.06.011.

McDonald, N., Timar, L., McDonald, G., & Murray, C. (2020). Better resilience evaluation: Reflections on investments in seismic resilience for infrastructure. *Bulletin of the New Zealand Society for Earthquake Engineering*, *53*, 203–214. http://dx.doi.org/10.5459/bnzsee.53.4.203-214.

Mechler, R. (2016). Reviewing estimates of the economic efficiency of disaster risk management: opportunities and limitations of using risk-based cost–benefit analysis. *Natural Hazards*, *81*, 2121–2147. http://dx.doi.org/10.1007/S11069-016-2170-Y/FIGURES/4.

Merz, B., Elmer, F., & Thieken, A. H. (2009). Significance of "high probability/low damage" versus "low probability/high damage" flood events. *Natural Hazards and Earth System Sciences*, *9*, 1033–1046. http://dx.doi.org/10.5194/NHESS-9-1033-2009.

Michel-Kerjan, E., Hochrainer-Stigler, S., Kunreuther, H., Linnerooth-Bayer, J., Mechler, R., Muir-Wood, R., et al. (2013). Catastrophe risk models for evaluating disaster risk reduction investments in developing countries. *Risk Analysis*, *33*, 984–999. http://dx.doi.org/10.1111/J.1539-6924.2012.01928.X.

Nan, C., & Sansavini, G. (2017). A quantitative method for assessing resilience of interdependent infrastructures. *Reliability Engineering & System Safety*, *157*, 35–53. http://dx.doi.org/10.1016/J.RESS.2016.08.013.

von Neumann, J., & Morgenstern, O. (2007). *Theory of games and economic behavior (60th anniversary commemorative edition)*: *vol. 9781400829460*, (pp. 1–741). Princeton University Press, http://dx.doi.org/10.1515/9781400829460.

OECD, The World Bank, & U. N. Environment (2018). Financing climate futures: Rethinking infrastructure. In *Financing Climate Futures*. Paris, France: OECD Publishing, http://dx.doi.org/10.1787/9789264308114-EN.

Ouyang, M. (2014). Review on modeling and simulation of interdependent critical infrastructure systems. *Reliability Engineering & System Safety*, *121*, 43–60. http://dx.doi.org/10.1016/J.RESS.2013.06.040.

Pagani, M., Monelli, D., Weatherill, G., Danciu, L., Crowley, H., Silva, V., et al. (2014). Openquake engine: An open hazard (and risk) software for the global earthquake model. *Seismological Research Letters*, *85*(3), 692–702. http://dx.doi.org/10.1785/0220130087.

Pagani, M., Monelli, D., Weatherill, G. A., & Garcia, J. P. (2014). *The OpenQuake-engine Book: Hazard*: *Tech. rep.*, Global Earthquake Model Foudation, URL https://cloud-storage.globalquakemodel.org/public/wix-new-website/pdf-collections-wix/publications/OQ%20Hazard%20Science%201.0.pdf Global Earthquake Model (GEM) Technical Report 2014-08.

Pagliara, F., & Zingone, M. (2023). Providing resilience due to adverse weather events: A cost-benefit analysis for the case of the Milan Malpensa airport in Italy. *Journal of Air Transport Management*, *113*, Article 102484. http://dx.doi.org/10.1016/J.JAIRTRAMAN.2023.102484.

Panteli, M., & Mancarella, P. (2017). Modeling and evaluating the resilience of critical electrical power infrastructure to extreme weather events. *IEEE Systems Journal*, *11*, 1733–1742. http://dx.doi.org/10.1109/JSYST.2015.2389272.

Petersen, M. D., Frankel, A. D., Harmsen, S. C., Mueller, C. S., Haller, K. M., Wheeler, R. L., et al. (2008). *Documentation for the 2008 update of the United States National Seismic Hazard Maps*: *Tech. rep.*, Reston, VA: United States Geological Survey, http://dx.doi.org/10.3133/OFR20081128, Open-File Report.

Porras-Alvarado, J. D. (2016). *A methodological framework for cross-asset resource allocations to support infrastructure management* (Ph.D. thesis), Austin, Texas: Department of Civil, Architectural and Environmental Engineering, University of Texas at Austin.

Rentschler, J., Avner, P., Marconcini, M., Su, R., Strano, E., Vousdoukas, M., et al. (2023). Global evidence of rapid urban growth in flood zones since 1985. *Nature*, *622*(7981), 87–92. http://dx.doi.org/10.1038/s41586-023-06468-9.

Rieger, M. O., Wang, M., & Hens, T. (2017). Estimating cumulative prospect theory parameters from an international survey. *Theory and Decision*, *82*, 567–596. http://dx.doi.org/10.1007/S11238-016-9582-8/METRICS.

Rinaldi, S., Peerenboom, J., & Kelly, T. (2001). Identifying, understanding, and analyzing critical infrastructure interdependencies. *IEEE Control Systems Magazine*, *21*(6), 11–25. http://dx.doi.org/10.1109/37.969131.

Santos, J. R. (2006). Inoperability input-output modeling of disruptions to interdependent economic systems. *Systems Engineering*, *9*, 20–34. http://dx.doi.org/10.1002/SYS.20040.

Scholten, L., Schuwirth, N., Reichert, P., & Lienert, J. (2015). Tackling uncertainty in multi-criteria decision analysis – An application to water supply infrastructure planning. *European Journal of Operational Research*, *242*, 243–260. http://dx.doi.org/10.1016/J.EJOR.2014.09.044.

Shreve, C. M., & Kelman, I. (2014). Does mitigation save? Reviewing cost-benefit analyses of disaster risk reduction. *International Journal of Disaster Risk Reduction*, *10*, 213–235. http://dx.doi.org/10.1016/J.IJDRR.2014.08.004.

Talebiyan, H., & Duenas-Osorio, L. (2020). Decentralized decision making for the restoration of interdependent networks. *ASCE-ASME Journal of Risk and Uncertainty in Engineering Systems, Part A: Civil Engineering*, *6*, Article 04020012. http://dx.doi.org/10.1061/AJRUA6.0001035.

The World Bank (2010). *Cost-benefit analysis in World Bank projects* (pp. 1–79). Washington D. C.: The World Bank Group, URL https://documents.worldbank.org/en/publication/documents-reports/documentdetail/216151468335940108/cost-benefit-analysis-in-world-bank-projects.

Thurner, L., Scheidler, A., Schafer, F., Menke, J. H., Dollichon, J., Meier, F., et al. (2018). Pandapower - An open-source Python tool for convenient modeling, analysis, and optimization of electric power systems. *IEEE Transactions on Power Systems*, *33*(6), 6510–6521. http://dx.doi.org/10.1109/TPWRS.2018.2829021.

Tversky, A., & Kahneman, D. (1992). Advances in prospect theory: Cumulative representation of uncertainty. *Journal of Risk and uncertainty*, *5*, 297–323. http://dx.doi.org/10.1007/BF00122574.

Wächter, A., & Biegler, T. L. (2006). On the implementation of an interior-point filter line-search algorithm for large-scale nonlinear programming. *Mathematical Programming*, *106*(1), 25–57.

Wang, S., Hong, L., & Chen, X. (2012). Vulnerability analysis of interdependent infrastructure systems: A methodological framework. *Physica A. Statistical Mechanics and its Applications*, *391*, 3323–3335. http://dx.doi.org/10.1016/J.PHYSA.2011.12.043.

Wise, R. M., Capon, T., Lin, B. B., & Stafford-Smith, M. (2022). Pragmatic cost–benefit analysis for infrastructure resilience. *Nature Climate Change*, *12*(10), 881–883. http://dx.doi.org/10.1038/s41558-022-01468-5.

Yang, R., Kiekintveld, C., Ordonez, F., Tambe, M., & John, R. (2011). Improving resource allocation strategy against human adversaries in security games. In *IJCAI proceedings-international joint conference on artificial intelligence, Vol. 22, No. 1* (p. 458). Barcelona.

Zhu, Q., & Leibowicz, B. D. (2022). A Markov decision process approach for cost-benefit analysis of infrastructure resilience upgrades. *Risk Analysis*, *42*, 1585–1602. http://dx.doi.org/10.1111/RISA.13838.